Solid Earth Discuss., 4, 315–361, 2012
www.solid-earth-discuss.net/4/315/2012/
doi:10.5194/sed-4-315-2012

Solid Earth
Discussions

Upper Pliensbachian – Toarcian (Jurassic) palaeoenvironmental perturbations in a temporal and regional context: an extended $^{87}Sr/^{86}Sr$, $\delta^{13}C$ and $\delta^{18}O$ belemnite isotope study from Bulgaria

L. S. Metodiev[1], I. P. Savov[2], D. R. Gröcke[3], P. B. Wignall[2], R. J. Newton[2], P. V. Andreeva[1], and E. K. Koleva-Rekalova[1]

[1]Geological Institute, Bulgarian Academy of Sciences, Acad. G. Bonchev Str. Bl. 24, 1113 Sofia, Bulgaria
[2]University of Leeds, School of Earth and Environment, Leeds LS2-9JT, UK
[3]Durham University, Department of Earth Sciences, Durham DH1 3LE, UK

Received: 3 February 2012 – Accepted: 6 February 2012 – Published: 13 February 2012

Correspondence to: I. P. Savov (i.savov@see.leeds.ac.uk)

Published by Copernicus Publications on behalf of the European Geosciences Union.

Abstract

The Upper Pliensbachian–Toarcian (Jurassic) sedimentological, palaeontological and geochemical (belemnite $^{87}Sr/^{86}Sr$, $\delta^{13}C$ and $\delta^{18}O$) record is examined in two Eastern Tethyan (Bulgarian) locations. This interval contains the well-known Early Toarcian ocean anoxic event (T-OAE) and its manifestation and temporal context is examined in Bulgaria. Many of the features characteristic for the SW European sections were identified: collapse of carbonate platform productivity at the Pliensbachian/Toarcian boundary, the T-OAE (a short pulse of anoxic deposition in the Falciferum ammonite Zone), an Early Toarcian rapid warming event seen in the belemnite $\delta^{18}O$ record that peaked around the Falciferum/Bifrons ammonite zonal boundary. The long-recognized positive $\delta^{13}C$ excursion in the late Falciferum ammonite Zone is also seen but a precursor, sharp $\delta^{13}C$ negative excursion seen around the Tenuicostatum/Falciferum ammonite zonal boundary in many organic carbon records is not evident in the belemnite data, a curious absence noted from other belemnite records. Subsequent fluctuations of the $^{87}Sr/^{86}Sr$, $\delta^{13}C$ and $\delta^{18}O$ suggest there may be a further perturbation of the global isotopic systems. On the other hand, belemnite Sr isotope values from Bulgaria are in accord with those seen in Western Europe and hence its value for chronostratigraphy.

1 Introduction

The majority of studies on the biogeochemical cycles of the Early Jurassic have been devoted to investigations of the Pliensbachian–Toarcian time slice. During this time interval there is a wide range of palaeontological, sedimentological and isotope evidence supporting the notion that a marine mass extinction event is associated with prominent $\delta^{13}C$ excursions, negative $\delta^{18}O$ shifts (e.g. warmer seawater temperatures or changes in the isotopic composition of seawater), a distinct shift in the seawater $^{87}Sr/^{86}Sr$ ratio, widespread anoxia, and substantial sea-level changes (e.g. Jenkyns, 1988; Jones et al., 1994; Sælen et al., 1996; Harries and Little, 1999; Hesselbo et al., 2000; McArthur et al., 2000; Jenkyns et al., 2002; Bailey et al., 2003; Wignall et al., 2005; Rosales et al., 2003, 2004; Kemp et al., 2005; Gröcke et al., 2007; Dera et al., 2009; Suan et al., 2010; Jenkyns, 2010; Dera et al., 2011). These major biogeochemical disturbances deeply affected both marine biota and global carbonate production in the shallow and deep ocean (Jones et al., 1994; Dera et al., 2009; Jenkyns, 2010; Al-Suwaidi et al., 2010; Gröcke et al., 2011; Izumi et al., 2011). A major palaeoceanographic phenomenon at this time – the Early Toarcian oceanic anoxic event (T-OAE) – may have been a driver of some of these changes (Jenkyns, 1988; Jones et al., 1994). Subsequently, global environmental conditions are considered to have remained relatively stable (Jenkyns, 1988; Jones et al., 1994; Jenkyns et al., 2002) although the late Toarcian Variabilis ammonite Zone recorded minor, short-term $\delta^{13}C$ and $\delta^{18}O$ oscillations in some locations (e.g. Wales, Jenkyns et al., 1997; Spain, Gómez et al., 2008; Bulgaria, Metodiev and Koleva-Rekalova, 2009, and Morocco, Bodin et al., 2010).It is unknown if these events record further global palaeoenvironmental changes and faunal turnover after the T-OAE and if they are discrete events or a consequence of the post-T-OAE stabilization (Gómez et al., 2008). Perhaps significantly, there is evidence for turnover and abundance-diversity variations in upper Toarcian fossil assemblages: these include the extinction of the ammonite subfamily Phymatoceratinae, the resurgence of the ammonite subfamily Harpoceratinae and the incoming in abundance of the ammonite families Grammoceratidae and Hammatoceratidae (Bécaud et al., 2005; Dera et al., 2010), as well as the turnover of brachiopods and small benthic foraminifers (Alméras et al., 1997; Ruget and Nicollin, 1997).

In order to better understand Late Pliensbachian – Toarcian palaeoenvironmental changes, a thorough investigation of key temperature and ocean chemistry sensitive isotope tracers is required. The marine $^{87}Sr/^{86}Sr$ record is buffered against restricted and short-term fluctuations in ancient seawater due to the long residence time of Sr in the oceans (e.g. McArthur et al., 2000), and provides a record of major plate-scale events, linked to variations in the marine Sr input-output fluxes (e.g. Peterman et al., 1970; Elderfield, 1986; Veizer et al., 1997; McArthur et al., 2000; Waltham and Gröcke,

SED
4, 315–361, 2012

2006). Jenkyns et al. (2002), among others, have shown that the Lower Jurassic Sr-isotope curve has a well-defined shape. However, the Late Toarcian portion of this curve is poorly defined and it is considered uneventful and of lesser use in evaluating palaeoenvironments compared to the Early Toarcian record. The same also holds true for the Late Toarcian δ^{13}C and δ^{18}O records (i.e. Gröcke et al., 2007).

The present study aims to decipher the variations of seawater ^{87}Sr/^{86}Sr, δ^{13}C and δ^{18}O and sedimentary record of the Late Pliensbachian – Toarcian interval. We use multiple lines of evidence from well-defined ammonite biostratigraphy, detailed lithology of fossil-bearing rocks, and the isotope record from well-preserved belemnite rostra from two sections located in the Teteven region of the Central Fore-Balkan Mountains in Bulgaria. Compared to some European Toarcian sections, the Bulgarian examples are thin, partly condensed, with stratigraphic hiatuses, and often sparsely fossiliferous. Nonetheless, they provide important information with regard to the T-OAE, and in the construction of Late Pliensbachian – Toarcian Sr, C, and O-isotope curves; thus to obtain a chemostratigraphic resolution superior to the Bulgarian ammonite zonal scheme.

2 Geological setting

2.1 Background geology and stratigraphy

The Jurassic sediments of the Teteven region (Central Fore-Balkan, Bulgaria) have long been known for their abundant and very diverse fossils. This particularly applies to the Lower Jurassic exposures, which have attracted much attention for more than a century now (e.g. Toula, 1881, 1889; Zlatarski, 1908; Cohen, 1931, 1932; Sapunov, 1969; Sapunov et al., 1971; Metodiev, 2008). Locally, these Lower Jurassic outcrops are considered to be an integral part of the most elevated segments of the Teteven Arch (Bonchev, 1971), which is a prominent positive structure of the Balkan Zone of the Balkan orogenic system (see Fig. 1a, b). Regionally, the Balkan orogenic system represents the northernmost part of the Alpine orogenic belt in Bulgaria that

SED
4, 315–361, 2012

was created during multiphase collisional and extensional tectonic events in the Late Palaeozoic to mid-Eocene (Zagorchev et al., 2009). According to Bonchev (1971), the Teteven Arch contains a basement of red Permian polymictic clastic sediments, associated with volcanoclastic rocks and acid tuffs, covered by dark-red polymictic clastic sediments of the Lower Triassic Petrohan Terrigenous Group. The Lower Triassic sediments are overlain by thick carbonates of the Middle Triassic Iskar Carbonate Group, which grade upward into the regressive carbonate facies of the Upper Triassic Moesian Terrigenous-carbonate Group. This variegated basement is covered unconformably by thick Jurassic successions that continue up to the Lower Cretaceous (Fig. 1b).

In the vicinity of the town of Teteven the Jurassic strata form a spectacular landscape on the northern slope of the Beli Vit River valley (Fig. 1c) and provide a continuous depositional record of the Jurassic (e.g. Sapunov, 1961, 1968, 1969; Shopov, 1970; Sapunov et al., 1971; Sapunov and Tchoumatchenco, 1989, and references therein). Mixed shallow- to medium-depth carbonates and siliciclastic sediments that were accumulated during an expanding marine transgression represent the Lower–Middle Jurassic rocks of the area. These deposits largely correspond to the Ozirovo and the Etropole Formations that span the Early Sinemurian to the Early Bajocian (Fig. 1d) (Sapunov and Tchoumatchenco, 1989).

The Ozirovo Formation is subdivided into three members, in ascending order: the Teteven, Dolni Loukovit and Boukorovtsi Members. The Teteven Member is a regionally extensive shallow-marine sequence of Early Sinemurian to Early Pliensbachian age, composed of a 10–30 m thick succession of alternating sandy bioclastic limestones, calcareous sandstones and silty marls with abundant bivalves, common brachiopods and scarce belemnite rostra. The Dolni Loukovit Member is a 30–80 m thick succession of ferruginized, sandy bioclastic limestones, of Early Sinemurian to Late Pliensbachian age. Above this the Boukorovtsi Member is a 20–40 m thick hemipelagic, irregular shale-marl-limestone alternation of Late Pliensbachian to Late Aalenian age. The uppermost Pliensbachian and Toarcian segment of the Boukorovtsi Member are the most fossiliferous (mainly ammonites and belemnites) and notably ooid-bearing. The rest of

SED
4, 315–361, 2012

the Boukorovtsi Member is monotonous with scarce fossils and the fossil assemblages are dominated by the pasichinal traces of *Zoophycos*.

The Ozirovo Formation is sharply overlain by the 150 m thick, poorly fossiliferous, deeper-water shales and siltstones of the Etropole Formation that ranges from the Late Aalenian to the end of the Middle Bajocian (Sapunov and Tchoumatchenco, 1989). The Lower–Middle Jurassic lithostratigraphy of the Teteven area displays uneven depositional rates that were highest in two intervals: the Sinemurian to Pliensbachian and the Aalenian to Middle Bajocian, with a markedly condensed Toarcian portion (Fig. 1d) reflecting an often interrupted sedimentary influx (Metodiev, 2008). The scarcity of Toarcian fossils prevents a high-resolution biostratigraphic subdivision and thus correlation with other coeval strata from elsewhere. In this study, we adopt the recently proposed Toarcian ammonite zonation for Bulgaria (Metodiev, 2008) that can be correlated with the NW European chart of Elmi et al. (1997) (Fig. 2).

2.2 Palaeogeography

In terms of palaeogeography, the Lower–Middle Jurassic rocks in the Teteven area represent inner shelf sediments deposited into a highly fragmented epicontinental basin of strait-like configuration (Zagorchev et al., 2009). It was developed onto the Moesian Platform due to early Jurassic extension and normal faulting in environments proximal to the southern Eurasian passive continental margin (Bassoulet et al., 1993; Fourcade et al., 1995). This basin was part of the wide north-western Peritethyan epicontinental sea, and there is general agreement that it was located in the Northern Hemisphere at a palaeolatitude between 33° N and 38° N (Dera et al., 2009, and references therein).

3 Materials and methods

This work is based on the study of petrographic samples, belemnite rostra, and ammonite specimens, which are part of the Bulgarian Geological Institute collections

SED
4, 315–361, 2012

(Coll. No. F.FSR.SR.2012.1). Twenty-three samples of the host rocks were taken for facies analysis and 48 belemnites (mostly *Dactyloteuthis* and *Acrocoelites*, and less commonly *Passaloteuthis* and *Gastrobelus*) were chosen for isotopic measurements. The petrographic thin sections were studied using conventional microscopy and represent each rock type recognized in the field. In general, the sampling density of the belemnites was in the range of a few vertical centimetres, depending on the amount and the density of occurrence of the belemnite rostra. For the purposes of our study, we collected 230 ammonites in order to give the best possible biostratigraphic subdivision and to supplement the available biochronostratigraphic database (Sapunov, 1968; Sapunov et al., 1971; Metodiev, 2008). Before the isotope measurements, belemnite rostra were carefully screened under plane light and cathodoluminescence for evidence of preservation, recrystallization, and luminescence characteristics. From each belemnite, a polished thick-section was prepared for a cathodoluminescence study and microsampling. After the assessment from cathodoluminescence, only the non-luminescent areas of the rostra interior were chosen and the sampling was carried out by using a dentist drill, avoiding rostra periphery, apical lines, portions of non-homogenous pattern, small veins and fractures filled with secondary calcite and borings.

Approximately 50 µg carbonate powder was collected for $^{87}Sr/^{86}Sr$ measurements and a minimum of 150 µg was used for $\delta^{18}O$ and $\delta^{13}C$ analyses. The $^{87}Sr/^{86}Sr$ measurements were performed at the Geochronology Laboratory of the School of Earth and Environment at the University of Leeds (UK). Each carbonate powder underwent a leaching procedure as recommended by Jones et al. (2000). Briefly, this procedure included the submergence of sample powders in 0.9 ml 18 MΩ water, addition of 0.2 ml of 0.4 M acetic acid and centrifuging for ∼5 min., followed by removal of up to 1 ml of the leached solution, in order for some of the insoluble residue to remain in the vial. To the insoluble residue, we added 1 ml of 1.7 M acetic acid until total dissolution was achieved. The solution was then evaporated to dryness at 80 °C for ∼1 h. The white carbonate residues were re-dissolved in 1.5 ml of 2.5 M HCl solution and centrifuged

SED
4, 315–361, 2012

again prior to the column separations. Strontium was separated via standard chromatography method using Eichrom Sr-resin and the purified solution was subsequently dried at 80 °C. The evaporated Sr-extracts were re-dissolved in ultrapure weak HCl acid and added onto tungsten wire with a previously applied and gently dried $TaCl_5$ ionization cocktail. The $^{87}Sr/^{86}Sr$ ratios were measured on Thermo-Finnigan Triton-series thermal ionization mass spectrometer. To achieve maximum precision and accuracy (see McArthur et al., 2000) the ^{88}Sr signal was bracketed between 5 and 8V and a minimum of 200 isotope ratios were collected. The internal precision was maintained between 1.3×10^{-6} and 7.1×10^{-6}. Analytical precision was monitored by repeated analysis of the standard, NBS-987. During analysis of the samples, the mean measured value obtained for NBS-987 was 0.710254 (2σ, $n = 31$). All measured $^{87}Sr/^{86}Sr$ data has been normalized to NBS-987 literature value of 0.710248 (McArthur et al., 2002). Total blanks were <2 ng Sr. Concentrations of Rb were too low to require correction for radiogenic ^{87}Sr.

The $\delta^{18}O$ and $\delta^{13}C$ analyses were performed in the Total Laboratory for Source Rock Geochronology and Geochemistry at the Department of Earth Sciences, Durham University. Approximately 200–250 µg of carbonate powder was placed in a glass vial. The sample vials were purged with He and subsequently injected with 103 % phosphoric acid to produce gaseous CO_2, while being maintained at 50 °C. Isotopic analysis was conducted using a Thermo Finnigan MAT 253 isotope-ratio mass spectrometer coupled with a Gas Bench II. Samples were calibrated against NBS-19 and LSVEC and isotopic data are reported against VPDB, with a 1σ precision error of 0.06 ‰ for C and 0.08 ‰ for O.

SED
4, 315–361, 2012

4 Description of the sections

4.1 Varbanchovets

The studied interval, located near the northern end of the town of Teteven (42°55′11′′ N; 24°16′16′′ E), is part of a thick section (>80 m) that spans the entire Lower Jurassic (Fig. 1c, d). The biostratigraphy has been previously studied by Sapunov (1961, 1968), Sapunov et al. (1971) and recently by Metodiev (2008). Here, the 3.3 m thick sequence of the Boukorovtsi Member of the Ozirovo Formation yielded 26 well-preserved belemnites and 150 ammonite specimens that enabled us to stratigraphically place it from the Lower Toarcian Tenuicostatum ammonite Zone (Semicelatum Subzone) to the Upper Toarcian Fallaciosum ammonite Zone (Figs. 2, 3, 4). The ammonite succession of this section was previously reported to extend from the Fallaciosum ammonite Zone onwards (Sapunov, 1968; Sapunov, et al., 1971), but this was not confirmed by our study. Due to no exposures and/or lack of both ammonites and belemnites, the beds below the Tenuicostatum ammonite Zone and above the Fallaciosum ammonite Zone were not sampled. The summarized bed-by-bed description of the section is included in Appendix A.

4.2 Babintsi

This is a newly discovered section located 2 km SW of the village of Babintsi and 6 km NW to the town of Teteven (42°56′46′′ N; 24°15′25′′ E) (Fig. 1c, d). It is a 3 m thick succession of the topmost beds of the Dolni Loukovit Member and the lower parts of the Boukorovtsi Member of the Ozirovo Formation (Figs. 5, 6). The age of the sampled interval was determined as extending from the Early Pliensbachian to post-Toarcian, but the lack of belemnites at the top made it impossible to determine if there are any strata younger than the Late Toarcian Fallaciosum ammonite Zone. About 80 ammonites were collected from 2 m thick sequence, and 22 well-preserved belemnite rostra were selected for isotope measurements. A summarized bed-by-bed description of the section is included in Appendix B.

SED
4, 315–361, 2012

5 Results and discussion

5.1 The biosedimentary evidence

5.1.1 Sedimentary record

Although thin, the clayey-carbonate successions of sections Varbanchovets and Babintsi represent good examples of Toarcian hemipelagic deposits. These sections record a carbonate crisis that is widely recorded in the Late Pliensbachian–Middle Bajocian interval in both Bulgaria and elsewhere in the north-western Tethyan domain of Europe (e.g. Tremolada et al., 2005). The two sequences comprise mostly marls and, to a lesser extent, finely-laminated, carbonate-free shales that alternate with thin bioclastic limestones. The non-winnowed limestone textures (see Fig. 6) and common marl beds suggest deposition in a relatively low-energy marine setting located below effective wave base. Marls dominate the Varbanchovets section suggesting that it was deposited in a more basinal setting than the Babintsi section, where carbonates are more common. The abundance of ammonites and belemnites, as well as crinoids, ostracods and brachiopod biodetritus, indicates an open-marine setting with normal salinity and water circulation. Sporadic foraminifers (often with broken tests) are interpreted as being transported from a shallow marine environment. Iron ooids are very common in most of the studied limestones and marl beds, and they too are considered to be allochthonous grains transported from a shallow marine environment. The genesis of ooidal ironstones in marine environments are favoured by clastic sediment starvation, reworking and an iron-rich hinterland (Hallam and Bradshaw, 1979; Young, 1989; van Houten and Purucker, 1984; van Buchem and Knox, 1998); an interpretation in accord with that proposed by Nachev (1960) for the Bulgarian Lower Jurassic ooidal ironstones.

The thin Toarcian record from both sections suggests a sediment starved-shelf deposition during a transgressive episode (Fig. 3). This retrogradation is marked by physical evidence of oxygen-restriction in the Falciferum ammonite Zone (laminated shales in

SED
4, 315–361, 2012

the Varbanchovets section) and in the Bifrons to Thouarsense ammonite Zones enrichment of organic matter and pyrite aggregates suggests dysoxia. The Babintsi section lacks evidence for the oldest two Toarcian ammonite zones and the younger strata show no evidence for dysoxia in this shallower water section.

5.1.2 Ammonite biostratigraphy and taphonomy

The studied sections yield characteristic Toarcian ammonite taxa that are common throughout NW Europe, allowing correlation with other Toarcian successions (Fig. 2). The Late Pliensbachian age of the basal beds of Babintsi section was determined by the presence of large bivalves of the genus *Pseudopecten*. Most of the Toarcian ammonites belong to the Hildoceratidae (eight species of genera *Hildoceras* and *Harpoceras*, accompanied by occasional *Hildaites*, *Orthildaites*, *Pseudolioceras* and *Polyplectus*), followed by abundance by Grammoceratinae (eight species of genera *Podagrosites*, *Pseudogrammoceras* and *Grammoceras*), Dactylioceratidae (six species of genera *Dactylioceras*, *Zugodactylites*, *Catacoeloceras* and *Peronoceras*), and Phymatoceratidae (four species of the genus *Haugia*). The best-recorded ammonite assemblage is that of the Bifrons ammonite Zone which can be divided into subzones in both sections. The Thouarsense and Fallaciosum ammonite zones, and the Semicelatum Subzone of the Tenuicostatum ammonite Zone are clearly defined as well (Figs. 3 and 5). The Variabilis ammonite Zone at the section Babintsi has the best-preserved *Haugia* specimens known from Bulgaria, whereas the record of this zone in the Varbanchovets section is poor. The Falciferum ammonite Zone of the Varbanchovets section yielded few ammonites. The maximum thickness of the zones and subzones does not exceed 0.9 m (for the Semicelatum Subzone and the Bifrons ammonite Zone), while the rest of the recognized units cover thicknesses ranging between 0.2 and 0.5 m. It is interesting to note that from the Lower Toarcian to the Upper Toarcian there is a decrease in the thickness of zones/subzones and ammonite abundance (Figs. 3 and 5).

In accord with the condensed nature of deposition the state of ammonite preservation often indicates prolonged biostratinomic processes that affected their shells prior to final burial. Here we have adapted the approach of Fernández-López (1991, 1997) to evaluate the taphonomy of the ammonite fauna. Usually the ammonites have only partly preserved body chambers and consist of phosphatized internal moulds of partial or whole phragmocones that are commonly grouped into clusters of extremely high concentration. Other ammonites may have the same filling as the host rock or lack sedimentary infilling. The latter are rare and show much less deformation and damaged. More than 90 % of the ammonites from the Varbanchovets section are reworked, indicating low rates of sedimentation in this depositional setting. However, the proportion of reworked ammonites decreases upwards by a factor of three in the Varbanchovets section: from the Semicelatum Subzone to the Falciferum ammonite Zone, from the Bifrons to the Variabilis Zone, and upwards from the Thouarsense Zone (Fig. 3). This decline in reworking also coincides with a transition from fossiliferous beds to levels where the ammonites are particularly rare, and where only hollow ammonites were found, suggesting an increase of sedimentation rate. It is interesting to note that most of the reworked elements of the ammonite associations collected from Varbanchovets are immatures or microconchs, whereas complete adults and macroconchs are very rare. This particularly applies to the Lusitanicum and Bifrons Subzones where the ammonites consists almost entirely of very small individuals.

In contrast, the state of preservation of ammonites from Babintsi section is more variable. It appears that the reworked ammonites here are mainly associated with the marl intervals, whereas in the limestones they are rare. The ammonites of this sequence record all types of growth stages. The juvenile specimens were observed in limestone beds and occur as neomorphic-altered ammonite nuclei. The degree of post-mortem reworking in the Upper Toarcian ammonites appears to be higher compared with those from the Lower Toarcian.

5.1.3 Belemnite occurrence and preservation

Generally, the distribution patterns and the density of the belemnites found at both of the studied sections follow the characteristics for ammonites (Figs. 3 and 5). The levels with absent or rare belemnites are associated with the beds of little reworking of the ammonites, and usually the marly intervals are characterized by accumulations of abundant rostra that form distinct "belemnite battlefields" (sensu Doyle and Macdonald, 1997). Two types of belemnite battlefields are recognized. The first type consists of abundant belemnite associations of monospecific composition, a predominance of adult individuals, and a lack of orientation. In the Varbanchovets section this battlefield type was seen at the base and at the top of the Lusitanicum Subzone, and in the Bifrons Subzone, where it is composed of medium-sized *Passaloteuthis*. This battlefield type in the Babintsi section was identified in each marly bed from the top of the Bifrons Subzone to the middle of the Thouarsense ammonite Zone, where it consists of medium-sized *Acrocoelites*. The second type of belemnite battlefield records a more heterogeneous population structure and occasionally oriented rostra that are subordinate to the abundant ammonites. The Varbanchovets section is composed of small- to medium-sized *Dactyloteuthis* and *Acrocoelites* (Semicelatum Subzone), medium-sized *Passaloteuthis* and *Acrocoelites* (mid-Lusitanicum and Semipolitum Subzones), and medium-sized to large *Acrocoelites* and *Dactyloteuthis* belemnites (Thouarsense ammonite Zone). In the Upper Pliensbachian and Lower Toarcian for the Babintsi section, this battlefield type is made up of various sizes of *Acrocoelites* and *Dactyloteuthis*, occasional *Gastrobelus*, and, in the Upper Toarcian, by medium-sized *Dactyloteuthis* and *Acrocoelites* belemnites. Belemnite-poor strata from both sections contain belemnites from the genera *Acrocoelites* and *Dactyloteuthis.* The belemnites from the Varbanchovets section appear to be better preserved than those from Babintsi. The rostra from Babintsi are frequently bored and corroded, scavenged and broken, and most of them, especially the large individuals, showing intensive bioerosion that are a clear indicator of reworking.

SED
4, 315–361, 2012

L. S. Metodiev et al.

5.2 The isotope record

5.2.1 $^{87}Sr/^{86}Sr$ isotopic trends

The Sr isotope ratios measured on belemnites from Varbanchovets section show a general increase of $^{87}Sr/^{86}Sr$ ratios through the Toarcian (Table 1). The $^{87}Sr/^{86}Sr$ curve is composed of two distinct segments: a lower portion of less radiogenic values and upper portion of more radiogenic values separated by a section lacking well-preserved belemnites suitable for Sr isotope stratigraphy (Fig. 3). Two peaks are superimposed on the overall smooth shape of the Sr isotope curve at this section: one around the boundary between the Tenuicostatum and Falciferum ammonite zones and the other at the Bifrons/Semipolitum Subzone boundary, suggesting that the sequence might be highly condensed at these levels. Through the Tenuicostatum ammonite Zone (Semicelatum Subzone), the measured $^{87}Sr/^{86}Sr$ ratios range between 0.707088 and 0.707154, bordered at the bottom and at the top with values of 0.707177 and 0.707164 respectively. There is an exceptionally radiogenic $^{87}Sr/^{86}Sr$ ratio of 0.707371 recorded from a sample in the middle of the zone (Table 1).The samples from the base of the Falciferum ammonite Zone yield $^{87}Sr/^{86}Sr$ values that increase from 0.707101 to 0.707153. The interval assigned to the Bifrons ammonite Zone contains more radiogenic values with little variability, and $^{87}Sr/^{86}Sr$ ratios range between 0.707217 and 0.707244. Another unusually radiogenic ratio of 0.707388 was recorded from the base of the zone (Table 1). Up section, the samples from the Variabilis ammonite Zone continue with the same overall trend that is seen in the Bifrons ammonite Zone; that is trending towards more radiogenic Sr isotope ratios with values between 0.707236 and 0.707245. The $^{87}Sr/^{86}Sr$ ratios of belemnites from the Thouarsense ammonite Zone and the base of the Fallaciosum ammonite Zone are distinctly more radiogenic in respect to those from the underlying strata, and range between 0.707270 and 0.707312 (Fig. 3; Table 1).

Overall, the Sr isotope ratios measured on belemnites from the Toarcian portion of the Babintsi section are similar to those of the Varbanchovets section (Fig. 5; Table 2). However, a part of the Upper Pliensbachian was available and yielded $^{87}Sr/^{86}Sr$ values

SED
4, 315–361, 2012

that decline up section from 0.707134 to 0.707087. Above this there is a sharp increase in $^{87}Sr/^{86}Sr$ ratios (0.707230) across the hiatus that records the absence of the Tenuicostatum and Falciferum ammonite Zones as discussed above. The next interval of the Bifrons ammonite Zone contains minor fluctuations in $^{87}Sr/^{86}Sr$ ratios and a slight increase from 0.707230 to 0.707256 in the Lusitanicum Subzone, and weak decrease to 0.707214 in the Bifrons Subzone. The bottom of the Variabilis ammonite Zone yielded $^{87}Sr/^{86}Sr$ratios between 0.707236 and 0.707219 that subsequently rise sharply to 0.707311 in the middle of the Variabilis ammonite Zone and then sharply fall to 0.707220 (Fig. 5; Table 2). The uppermost portion of $^{87}Sr/^{86}Sr$ curve within the Thouarsense ammonite Zone and the bottom of the Fallaciosum ammonite Zone is composed by apparently more radiogenic values, ranging between 0.707291 and 0.707349. The topmost beds of the Babintsi section lack belemnites and hence no $^{87}Sr/^{86}Sr$ record is produced above the base of the Fallaciosum ammonite Zone.

5.2.2 Isotopic trends in belemnite $\delta^{13}C$

Both of the studied sections reveal the same broad trends: a marked Semicelatum Subzone-Falciferum ammonite Zone positive $\delta^{13}C$ excursion (with a maximum near the boundary of these zones), followed by a gradual decrease of $\delta^{13}C$ within the Bifrons ammonite Zone, slightly higher $\delta^{13}C$ and rather variable values in the Variabilis ammonite Zone and a gradual negative $\delta^{13}C$ shift toward the base of the Fallaciosum ammonite Zone. The $\delta^{13}C$ values of the Varbanchovets belemnites range between +0.84 ‰ to +3.25 ‰ (average of +1.8 ‰) (Fig. 3; Table 1). Initially, the $\delta^{13}C$ values display a rise from +0.95 ‰ at the base of the Semicelatum Subzone to +3.21 ‰, near the boundary of the Falciferum ammonite Zone; the latter representing the maximum $\delta^{13}C$ values from this section. This is immediately followed by an abrupt fall of $\delta^{13}C$ reaching a low value of1.1 in the Falciferum ammonite Zone. The $\delta^{13}C$ ratios then rise again before showing a long-term decline in the Upper Toarcian to values between +1 ‰ and +2 ‰ (Fig. 3). There is possibly a small positive excursion at the base of the Bifrons Subzone. The carbon isotope data from Babintsi show similar overall values to the Varbanchovets section with the exception of lower values in the Thouarsense ammonite Zone (Fig. 5, Table 2). The Variabilis ammonite Zone, sampled in more detail at Babintsi, also shows several oscillations following a broad trough in the Bifrons ammonite Zone.

5.2.3 Isotopic trends in belemnite δ^{18}O

The overall δ^{18}O evolution from the studied sections reveals relatively large variability of about 3, with an average value of −2 ‰ (Figs. 3 and 5; Tables 1, 2) and generally inverse correlation with the δ^{13}C isotope record for the same sections and same belemnite specimens. This is best seen in the Varbanchovets data where there is a clear Semicelatum Subzone to Lusitanicum Subzone negative δ^{18}O excursion that attains a maximum negative shift from −0.73 ‰ to −3.75 ‰ near the base of the Lusitanicum Subzone (Fig. 3; Table 1). This is followed by a trend to more enriched δ^{18}O values (ranging between −2.99 ‰ and −1.46 ‰), though they do not retain the values seen in the Tenuicostatum ammonite Zone (from −0.81 ‰ to −2.62 ‰). In the Babintsi section a significant part of the δ^{18}O record is missing at the major Pliensbachian/Toarcian boundary hiatus. Above this level the δ^{18}O values are more stable until the Variabilis ammonite Zone when they fall to lighter values in the later part of the zone before returning to somewhat variable but heavier values (Fig. 5).

5.2.4 Palaeotemperature variations derived from δ^{18}O

Palaeotemperatures shown on Tables 1 and 2 were calculated assuming that the belemnite calcites collected in the Toarcian deposits of the two studied sections are diagenetically unaltered and were precipitated in equilibrium with ambient seawater (e.g. Sælen et al., 1996; Jenkyns et al., 2002; Rosales et al., 2003, 2004). It is also assumed that during the time interval of these sections the oxygen isotope value of the seawater, and salinity remained relatively constant. The calculated temperatures from the belemnite rostra used the equation of Anderson and Arthur (1983), which

SED
4, 315–361, 2012
Toarcian belemnite isotope study from Bulgaria
L. S. Metodiev et al.

represents a modified equation of that provided by Craig (1965):

$$T(^{\circ}\mathrm{C}) = 16.0 - 4.14(\delta_c - \delta_w) + 0.13(\delta_c - \delta_w)^2 \quad (1)$$

where δ_c is δ^{18}O (‰PDB) of the sample, and δ_w equals the oxygen isotopic composition of the seawater which the calcite was precipitated from and in this study a value of −1 ‰ (SMOW) has been adopted (as suggested by Shackleton and Kennett, 1975).

The calculations from the δ^{18}O dataset of the Varbanchovets section yielded a succession of warming and cooling episodes during the Toarcian. At the lowermost Toarcian Semicelatum Subzone, the obtained palaeotemperatures are not unusual for this palaeo-latititude of ~35° N. Higher in the section, however, there is a record of rapid warming at the base of the Bifrons ammonite Zone, where the highest calculated palaeotemperature reaches 28.4 °C (Table 1). Following this warm interval seawater temperatures rapidly decrease in the Variabilis ammonite Zone to ~18.6 °C and remain only slightly warmer than this for the remainder of the Toarcian with the exception of a warming pulse in the Semipolitum Subzone which reached 24 °C.

Surprisingly, the Toarcian palaeotemperature calculations from Babintsi belemnites produced different values with a prolonged phase of stability around 21 °C followed by warmer values, especially in the Variabilis ammonite Zone when palaeotemperatures reached 26 °C (Table 2). The Babintsi section also yielded palaeotemperatures for the latest Pliensbachian, which produce very low values and a minimum of 9.8 °C.

5.2.5 The relative duration of ammonite zones and absolute age assessment

McArthur et al. (2000) studied the Sr isotope variations in Late Pliensbachian and Toarcian sediments from the Yorkshire coast of England. They demonstrated that if the rate-of-change of marine ^{87}Sr/^{86}Sr and the sedimentation rate remain constant for a given stratigraphic interval, then the change of ^{87}Sr/^{86}Sr with time is very close to being linear. This linear relationship can be utilized to estimate the relative durations of geological events preserved by the sedimentological record and the slope of the regression line enables the calculation of absolute ages. In the studied sections we found sedimentological discontinuities that are the product of particularly low sedimentation rates and that unfortunately could not be considered constant with time. Therefore, the measured $^{87}Sr/^{86}Sr$ ratios from the Varbanchovets and Babintsi sections were grouped into five linear segments, where the rate of change of $^{87}Sr/^{86}Sr$ is assumed to remain constant with stratigraphic level. Apportion of these segments was constructed according to the stratigraphic level of the samples: Upper Pliensbachian beds, Semicelatum Subzone interval, Falciferum ammonite Zone bed, Bifrons ammonite Zone succession and Variabilis-base Fallaciosum ammonite Zone intervals. Each segment was modeled by linear regression analysis, excluding samples that deviate from the main $^{87}Sr/^{86}Sr$ trend by $> 10^{-5}$ and therefore may have been (diagenetically?) modified. Absolute ages have been assigned to each belemnite specimen (see Tables 1 and 2; Fig. 7) using 183.6 +1.7/−1.1 Myr as the Pliensbachian-Toarcian boundary based on the U-Pb dating of volcanic ash layers from that boundary and also based on ammonoid dating from the North American Cordillera (Pálfy and Smith, 2000). In Fig. 7 the Bulgarian results are compared with the well-studied Sr isotope fluctuations reported from England (McArthur et al., 2000; Jenkyns et al., 2002). The comparison between the Bulgarian and the British sections reveal several important insights:

1. Overall the duration of the British Toarcian ammonite zones based on Sr isotope stratigraphy (McArthur et al., 2000) appears to be in good agreement with the results obtained from the Lower Jurassic sections of Central Fore-Balkan Mountains of Bulgaria (this study).

2. The non-deposition recorded at the Pliensbachian/Toarcian boundary in Babintsi section is estimated to have lasted in access of 2 Myr (from 184.27 to 181.80 Ma).

3. The Upper Pliensbachian part of Babintsi section has been assigned to a time span from 184.66 to 184.27 Ma, corresponding to the mid-Apyrenum Subzone.

4. The sampled interval of the Semicelatum Subzone of Varbanchovets section is found to be incomplete and representing only the last 0.06 Ma of the Semicelatum Subzone.

5. Although only a few belemnite specimens were discovered from the Falciferum ammonite Zone of the Varbanchovets section, they allowed us to attribute the basal 15 cm of the lower Serpentinum Subzone of the Falciferum ammonite Zone (Serpentinum Subzone in Bulgaria = Exaratum Subzone in Yorkshire). Considering the absolute ages calculated from the uppermost and the lowermost specimens of the Semicelatum Subzone and the Bifrons ammonite Zone, the duration of the Falciferum ammonite Zone in Varbanchovets section is found to be 1.49 Ma, and consequently the sedimentation rate appears to have been extremely low – in the order of 4 cm Ma^{-1}.

6. The calculations based on the Sr isotope data from both Babintsi and Varbanchovets sections revealed the Bifrons ammonite Zone lasting about 0.47 Myr. Thus, the subzonal division used in Bulgaria for this particular zone does not correspond to that in Yorkshire (and probably elsewhere), and future correlations at subzonal level involving the Bifrons ammonite Zone should be conducted with extra caution.

7. The Variabilis ammonite Zone in the Bulgarian sections appears to have lasted from 181.43 to 181.22 Ma, i.e. only 0.02 Ma longer when compared to the same zone in the Yorkshire coast sections (McArthur et al., 2000).

8. The Thouarsense/Fallaciosum boundary of the Bulgarian sections can be roughly placed at 180.99 Myr. The data density around this interval is too low in the Bulgarian sections, but the limited data points indicate quite a good agreement with the general trend toward more radiogenic $^{87}Sr/^{86}Sr$ recorded in the Yorkshire coast sections.

The differences observed in the durations of the various ammonite zones pose a problem. Taking the principle that the Toarcian was a time of great climatic change and thus caused environmental stress on seawater biota, it might be expected that the relative duration of the ammonite zones is a function of the degree of the environmental

SED
4, 315–361, 2012

pressure onto the aquatic ecosystems. Hence, the proposed reduction in the duration of the ammonite zones could be a consequence of even greater climate perturbation(s).

6 Encapsulation

The Bulgarian isotopic data provides us with information on the Late Pliensbachian–Toarcian sedimentary history of this eastern-central Tethyan region, which can be compared with better-known Early Toarcian records from the western Tethyan. Overall this will generate a better temporal coverage of the Toarcian in Europe.

6.1 Late Pliensbachian

Although this interval was only sampled at Babintsi, the belemnites from this section yield low palaeotemperatures that concord with the idea of a severe cool episode in the Late Pliensbachian (e.g. Bailey et al., 2003; Rosales et al., 2004; Gómez et al., 2008; Suan et al., 2010, 2011).Widespread evidence for a Pliensbachian/Toarcian sequence boundary suggests the cooling culminated in glacio-eustatic regression (e.g. Guex et al., 2001; Suan et al., 2010).

6.2 Early Toarcian

The Bulgarian sections record many of the same features seen elsewhere in Tethys. A base-level rise coincided with a crisis in platform carbonate deposition with the result that a hiatus is developed in shallow platform locations (Babintsi) whilst condensed, marly sediments with Fe ooids developed in deeper-water sections (e.g. Varbanchovets). In the latter location, the presence of finely laminated shales in the bottom of the Falciferum ammonite Zone (Fig. 3) is a clear a manifestation of the T-OAE and it provides the most easterly Tethyan record of this event.

SED
4, 315–361, 2012

The T-OAE also coincided with the onset of a rapid rise of $^{87}Sr/^{86}Sr$ ratios and carbon isotope shifts that include a controversial negative $\delta^{13}C$ excursion near the Tenuicostatum/Falciferum zonal boundary followed by a return to heavier values in the later Falciferum and early Bifrons ammonite Zones (Fig. 8; Jenkyns, 1988; Sælen et al., 1996; Hesselbo et al., 2000; McArthur et al., 2000; Jenkyns et al., 2002; Bailey et al., 2003; Rosales et al., 2003, 2004; Kemp et al., 2005; van de Schootbrugge et al., 2005; Wignall et al., 2006; Svensson et al. 2007; Dera et al., 2009, 2011; Gröcke et al., 2009, 2011; Suan et al., 2010; Isumi et al., 2011).

The Sr isotope curve from the Bulgarian sections confirms that produced from other European records, although the absence of suitable belemnites in the upper Falciferum ammonite Zone makes it difficult to precisely locate the inflection point in the $^{87}Sr/^{86}Sr$ curve (e.g. McArthur et al., 2000; Gröcke et al., 2007). In contrast the belemnite $\delta^{13}C$ record shows a ~2 ‰ positive excursion in the Toarcian, but the precursor negative excursion is absent (Fig. 8). This negative excursion has been recorded in sedimentary organic carbon and carbonate from various sections in Europe (e.g. Hesselbo et al. 2000, 2007; Schouten et al., 2000; Kemp et al., 2005; Suan et al., 2010, 2011). It has also been recorded in terrestrial organic matter thus showing that the oceanic and atmospheric carbon isotope cycle was affected (e.g. Hesselbo et al., 2000, 2007; Caruthers et al., 2011). The failure of the belemnite calcite record to reveal this excursion has been noted previously and widely debated (van de Schootbrugge et al., 2005; McArthur, 2007), although the precise mechanism of why this is the case is still unknown. The data presented indicate that the lack of a negative $\delta^{13}C$ excursion in belemnites is not a regional or taxon-specific signal but rather a consistent feature of this group. Additional global records of the $\delta^{13}C$ excursion have been produced confirming the hypothesis that the T-OAE is associated with a major negative carbon isotope excursion (e.g. Al-Suwaida et al., 2010; Caruthers et al., 2011; Gröcke et al., 2011; Isumi et al., 2011)

Belemnites have also provided a palaeotemperature record for the Toarcian interval, notably from Germany, Spain and the UK, that suggests a rapid temperature rise in

SED
4, 315–361, 2012

the Tenuicostatum–Falciferum ammonite Zones (Fig. 9; Bailey et al., 2003; Gómez et al., 2008; Gómez and Goy, 2011). The Bulgarian belemnite data produce comparable palaeotemperatures and the trends to those recorded in the western Tethys (Fig. 9).The culmination of this trend occurred around the Falciferum/Bifrons ammonite Zones boundary; similar palaeotemperatures are also recorded in Panthalassa (Gröcke et al., 2007). In detail, our data suggests there were higher-order palaeotemperature oscillations in the Tenuicostatum ammonite Zone superimposed on the overall warming trend (Fig. 9), a pattern also produced in other $\delta^{18}O$ records from belemnites (Gómez et al., 2008) and brachiopods (Suan et al., 2010). A recent study from northern Siberia notes the abundance of the thermophyllic pollen genus *Classopollis* in the early Falciferum to early Bifrons Biochrons as evidence of a severe warming event (Suan et al., 2011), suggesting that this Early Toarcian trend was a global phenomenon.

6.3 Late Toarcian

The re-establishment of platform carbonate productivity ensured a more complete Toarcian record in Bulgarian shallow-water sections, such as at Babintsi, whilst in deeper-water sections an increase in sedimentation rates reduced the degree of seafloor reworking of ammonites. Nonetheless iron ooids, considered to be the product of prolonged exposure on the seafloor, are common in both sections.

In Western Europe this interval sees the continued rise of $^{87}Sr/^{86}Sr$ (McArthur et al., 2000), although the carbon isotope curve is more complex: stable from Mochras Farm Borehole, Wales (Jenkyns et al., 2001), and declining trend in belemnites from Rodiles-Santa Mera, Spain (Gómez et al., 2008), Yorkshire and Dorset belemnites, UK (Jones et al., 1994). In general the Bulgarian record matches these trends although there is the suggestion of discrete events within the interval of the Variabilis–Thouarsense ammonite Zones. With the resolution of our data it is difficult to distinguish a clear pattern, thus $\delta^{13}C$ values show a possible negative excursion in the Thouarsense ammonite Zone, $\delta^{18}O$ values show a warming peak in the Variabilis ammonite Zone and substantial oscillations of the $^{87}Sr/^{86}Sr$ record implies sedimentary condensation and/or diagenetic alteration. All these observations require verification with more detailed studies of preferably more expanded sections, but the available data suggests similar trends are also present in western European sections (Figs. 8 and 9).

7 Conclusions

We studied the Lower Jurassic (Upper Pliensbachian–Toarcian) sedimentological, palaeontological and isotope (belemnite $^{87}Sr/^{86}Sr$, $\delta^{13}C$ and $\delta^{18}O$) record in two Eastern Tethyan hemipelagic successions in Bulgaria. We found that in the Central Balkan Mountains of Bulgaria this interval contains the well-known Early Toarcian ocean anoxic event (T-OAE). We have studied its manifestation and temporal context via study of its fossil and sedimentological record combined with the isotope systematic (C, O and Sr) measured in belemnite rostra. Many of the features of this event seen in other European locations were recognized:

1. A crisis in platform carbonate deposition at the Pliensbachian/Toarcian boundary, recorded by a 2 Ma hiatus in the shallow water sedimentary succession (missing are latest Pliensbachian and the Tenuicostatum and the Falciferum ammonite Zones),

2. The presence of short pulse of anoxic deposition during the early Falciferum ammonite Zone in finely laminated shales representing the deeper water succession.

3. The T-OAE coincided with the onset of rapid rise of $^{87}Sr/^{86}Sr$ ratios and $\delta^{13}C$ shifts that include a controversial negative $\delta^{13}C$ excursion near the Tenuicostatum/Falciferum zonal boundary, followed by a return to heavier $\delta^{13}C$ values in the late Falciferum and early Bifrons ammonite Zones.

4. An Early Toarcian rapid warming event was recorded in the belemnite $\delta^{18}O$ record. This worming appears to have peaked around the Falciferum/Bifrons

SED
4, 315–361, 2012

zonal boundary. Bulgarian belemnite data appears to provide palaeotemperature akin to trends recorded by western Tethys sections. Our new data from the Tenuicostatum ammonite Zone suggests that super imposed on the overall warming trends were higher-order palaeotemperature oscillations.

5. The good quality of our Sr isotope measurements enabled us to estimate the relative durations of geological events preserved by the sedimentological record of our sections. The Sr isotope systematics of the Bulgarian sections appear to match the well known smooth rise of $^{87}Sr/^{86}Sr$ ratios from the Pliensbachian/Toarcian boundary upwards. However, there is a suggestion of several discrete events within the Upper Toarcian interval covering the Variabilis–Thouarsense ammonite Zones. With the resolution of our data it is difficult to distinguish a clear pattern, thus $\delta^{13}C$ values show a possible negative excursion in the Thouarsense ammonite Zone, $\delta^{18}O$ values show a warming peak in the Variabilis ammonite Zone and substantial oscillations of the $^{87}Sr/^{86}Sr$ record implies possible sedimentary condensation and/or diagenetic alteration. All these observations require confirmation from additional studies of preferably more expanded sections, but the data available suggests similar trends are also present in several well-studied western European sections.Using the $^{87}Sr/^{86}Sr$ isotope ratios we found that the duration of the Toarcian ammonite zones from the studied sections of Central Fore-Balkan Mountains appear to be in good agreement with the results obtained from Yorkshire Coast in the UK.

Appendix A

Detailed description of sedimentary beds from section Varbanchovets

No. 5 (0.50 m). Dark-grey ferruginous marls, parallel bedding and laminated on a cm scale, with presence of many irregularly clustered iron ooids. The marls (Fig. 4a) are composed of clayey-carbonate matrix, containing poorly sorted and randomly dispersed broken skeletal grains (common crinoids, scarce ostracods and foraminifers), clastic in origin, and angular- to sub-rounded quartz and feldspar grains, and single muscovite flakes. Occasionally, finely disseminated pyrite grains may also be found. The ooids are usually deformed, phosphatized and of various shapes and sizes. Sparse, phosphatized or pyritized phragmocones of *Pseudogrammoceras* and occasional large belemnite rostra occur.

No. 4 (0.60 m). Light yellow-brownish ferruginous marls, with scattered deformed iron ooids (Fig. 4b). Common clastic quartz and feldspar, and less common muscovite and pyrite grains are mixed with bioclasts (mostly crinoids, sparse ostracods and foraminifers), all dispersed in carbonate-clayey matrix. The ammonite assemblage is fairly poor and represented by reelaborated phosphatized phragmocones of *Podagrosites*, *Grammoceras*, early *Pseudogrammoceras* and some *Catacoeloceras*, as well as a few hollow ammonites of *Haugia*. Belemnite rostra are common, occasionally oriented, and somewhat crushed and re-jointed by post-depositional cementation.

No. 3c (0.50 m). Grey ooid-bearing marls with poorly sorted bioclasts (crinoids, brachiopods, ostracods and single foraminifers), deformed and randomly dispersed phosphatized or carbonatized iron ooids in calcareous-clayey matrix (Fig. 4c, d). Angular to slightly rounded clastic quartz and feldspar grains with silt to fine sand size as well as rock fragments and pyrite were also discovered. The fossil assemblage consists of abundant belemnite rostra of various sizes with no orientation at the top of this bed and often oriented at the base. Rare finds of reelaborated ammonites of *Zugodactylites* and *Hildoceras* are preserved as phosphatized internal moulds of incomplete phragmocones.

No. 3b (0.20 m). Highly fossiliferous and ooid-bearing limestones (bioclastic wackestones with iron ooids, Fig. 4e),dark grey, yellowish when weathered. This bed consists of micritic/microsparitic matrix, comprising poorly sorted bioclasts

SED
4, 315–361, 2012

(crinoids, brachiopods, ostracods, and single foraminifers), iron ooids (some of them partly or completely replaced by sparry calcite), angular clastic non-carbonate grains (e.g. quartz and feldspar) of silt to fine sand size, and fine pyrite. It displayed a high value of fossil packing as being extremely rich in ammonites and less loaded in belemnites. Ammonites appear generally scattered throughout the bed, but sometimes particular pattern of clustering can be recognized. The ammonite assemblage is composed of reelaborated phosphatized immatures of *Hildoceras*. Microconchs of this genus are also identifiable. Immatures and microconchs of *Harpoceras*, *Pseudolioceras*, and *Dactylioceras (Dactylioceras)* may also be present.

No. 3a (0.20 m). Dark grey to bluish marls, with common deformed iron ooids and small phosphate nodules (1–5 cm in size). The rocks are composed of calcareous-clayey matrix, comprising angular to sub-rounded clastic grains of quartz, feldspar and lithoclasts with silt to fine sand size. Also present are rare bioclasts of crinoids, thin-shelled ostracods, brachiopods and single foraminifers (Fig. 4f). Ammonite record consists of common reelaborated immatures of *Hildoceras*, frequent small *Harpoceras*, and few *Dactylioceras (Dactylioceras)* and *Orthildaites*. The ammonites appear as phosphatized internal moulds, blended with abundant belemnite rostra that seem to be of monospecific assemblage.

No. 2 (0.40 m). Brown-ochre in colour shales, commonly showing wavy and fine (mm-scale) lamination. This interval is composed of ferruginized clayey matrix with small amount of clastic non-carbonate grains and bioclasts (Fig. 4g). The latter include echinoid spines, foraminifers, ostracods and crinoids. Some bioclasts are characterized by intra-granular pores filled with pyrite. Uncommon and fragmentary micritic or pyritic internal moulds of *Harpoceras* and *Hildaites* were found. Whole belemnites are rare, but well preserved when found. Usually the belemnite rostra are fragmentary and either encrusted by strongly oxidized and mm- in size pyrite or they were completely destroyed transformed into small pyrite tubes.

SED
4, 315–361, 2012

No. 1d–a (0.90 m). Black, ooid-bearing marls, interbedded with dark grey ooid-bearing bioclastic limestones. The marls contain common poorly sorted bioclasts (crinoids, brachiopods, echinoids, thin-shelled ostracods and foraminifers), scattered clastic angular quartz and feldspar grains. The limestones consist of clay-rich micritic/microsparitic matrix (Fig. 4h), with recrystallized skeletal grains (some crinoids, foraminifers and fine shell debris) and terrigenous non-carbonate grains (quartz, feldspar and deformed iron ooids). At several locations we found many small cubic pyrite crystals. These beds yielded the main portion of ammonites from this interval: several small planulates of *Dactylioceras (Orthodactylites)* preserved as phosphatized phragmocones with partly preserved body-chambers. Belemnites with no apparent orientation also appear to be very common, especially in the upper beds.

Appendix B

Detailed description of sedimentary beds from section Babintsi

No. 3b (0.20 m). Grey-yellowish ferruginized marls containing phosphatized internal moulds of incomplete phragmocones of common *Pseudogrammoceras* and single *Polyplectus*. The base of the bed contains abundant belemnites of different shapes and sizes with no current orientation, whereas the upper part of the bed is depleted in belemnite rostra.

No. 3a (0.50 m). Alternation of thin- to medium-bedded dark grey limestones with thin grey marls. The limestones (bioclastic wackestones and wackestones/packstones with iron ooids) consist of poorly sorted and randomly dispersed skeletal grains (mainly crinoids, common ammonite nuclei, and rare brachiopods, ostracods and foraminifers) within a clay-rich micritic or microsparitic matrix (Fig. 6a). Variable amount of iron ooids (<5–30 %) with carbonatized or well-preserved cortices are also common. The ooid nuclei are represented by broken ooid individuals (Fig. 6b) and to a lesser extent

SED
4, 315–361, 2012

of crinoid bioclasts, rare clastic angular quartz and feldspar grains. The marls contain sub-rounded quartz grains of silt size, muscovite flakes and bioclasts of crinoids and sponge spicules included in calcareous-clayey matrix. This sequence preserved a mixed ammonite-belemnite association of abundant belemnite rostra from heterospecific assemblage and common, reelaborated early *Pseudogrammoceras*, few ammonite species of *Grammoceras* and many *Podagrosites* and *Haugia* ammonites. The ammonites are preserved as phosphatized internal moulds displaying various sizes and maturity. Most of the fossils found in these beds were not deposited in situ.

No. 2c (0.45 m). Dark grey medium-bedded limestones (bioclastic wackestones and wackestones/packstones with iron ooids), intercalated by thin grey marls. The limestones are composed of micritic matrix with many crinoid bioclasts of various sizes, associated with rare ammonite nuclei, ostracods, foraminifers and brachiopods (Fig. 6c). The iron ooids are not uncommon (<5–15 %) vary in size between 0.30 and 0.70 mm and have superficial or normal ooid cortices. The latter are partly or completely carbonatized (Fig. 6d). Some external ooid shapes are strongly distorted. The non-carbonate supply consists of rare angular quartz grains and lithoclasts of silt to very fine sand size. Lithologically, the marls are identical to those described from bed 3a. This interval preserved relatively rich and diverse ammonite association, mainly of the genera *Hildoceras* and *Harpoceras*, single specimens of *Peronoceras* and *Zugodactylites*, and subordinate amount of belemnite rostra. The ammonites from marly horizons are reelaborated, whereas those extracted from the limestones seem to have been fossilized in situ. Belemnites appear mainly from the intercalated marls, as often oriented guards from the higher beds, and of no current orientation at the bottom of this sequence.

No. 2b (0.20 m). Black, ooid-bearing limestones (bioclastic wackestones) with clay-rich micritic/microsparitic matrix. These sediments contain poorly sorted crinoids (0.10 to 2.00 mm), sporadic brachiopods and ostracods, some ammonite nuclei,

SED
4, 315–361, 2012

as well as iron ooids (10 to 30 %), with highest density in the middle of the bed. Occasionally we also observed clastic angular quartz grains with silt to very fine sand sizes. Most of the iron ooids are characterized by normal ooid cortices which are composed of yellow-brown to dark brown ferruginous laminae with well-preserved concentric layering. Locally, external parts of some cortices are built up of carbonate layers with radial microfabric (Fig. 6e).Ooids vary in size from 0.3 mm to 1.6 mm, and have ellipsoidal, subsphaeroidal or irregular shapes. Some ooids are carbonatized (Fig. 6f) or may display deformed external structures. Broken, distorted (Fig. 6g) and pitted ooid types were discovered too. This bed contains plenty of adult macroconchs of *Hildoceras* and belemnites.

No. 2a (0.50 m). Alternation of thin-bedded dark grey to yellowish (when weathered) limestones and dark grey to black marls. The limestones (clayey-bioclastic wackestones and bioclastic wackestones/packstones) (Fig. 6h), contain poorly sorted crinoids grains (0.25 to 0.90 mm), brachiopod shells (ranging from 0.30 mm to 1.40 mm) and single ostracods, echinoid spines and foraminifers. Rare silt-sized clastic quartz grains and randomly distributed iron ooids are also observed, scattered within clay-rich micritic matrix. This finely bedded succession is fossil-bearing at the top and at the base, with an intermediate interval of 15 cm with no fossils. In this level the limestone interbeds have a lumpy appearance and usually grade into the marls. The marls from the top yielded the evidence for the incoming with abundance of *Hildoceras*, as reelaborated small phragmocones, mixed with scattered belemnites. Although thin, the marls from the base hold abundant large bivalve specimens of *Pseudopecten*, accompanied with occasional belemnites.

No. 1 (0.15 m). Grey-pink, medium-bedded and ferruginized limestones, occasionally recrystallized (bioclastic wackestones). No belemnites were found in this bed, but disarticulated and occasionally whole specimens of *Pseudopecten* are not uncommon.

SED
4, 315–361, 2012

Acknowledgements. We thank Bob Cliff for help and advice during the Sr isotope sample preparations and TIMS measurements. Iliya Dimitrov and Vasil Sirakov helped with the sample collection during fieldwork in Bulgaria. The stable isotope portion of this research was made possible by a NERC (NE/H021868/1) grant to DRG. Technical support at Durham University was provided by Joanne Peterkin.

References

Alméras, Y., Boullier, A., and Laurin, B.: Brachiopodes, in: Biostratigraphie du Jurassique ouest-européen et méditerranéen: zonations parallèles et distribution des invertébrés et microfossiles, edited by: Cariou, E. and Hantzpergue, P., Bull. Centre Rech. Explor. Prod. Elf Aquitaine 17, 169–195, 1997.

Al-Suwaidi, A. H., Angelozzi, G. N., Baudin, F., Damborenea, S. E., Hesselbo, S. P., Jenkyns, H. C.,Mancenido, M. O., and Riccardi, A. C.: First record of the Early Toarcian OceanicAnoxic Event from the Southern Hemisphere, Neuquen Basin, Argentina, J. Geol. Soc. London, 167, 633–636, doi:10.1144/0016-76492010-025, 2010.

Anderson, T. F. and Arthur, M. A: Stable isotopes of oxygen and carbon and their application to sedimentologic and palaeoenvironmental problems, in: Stable isotopes in sedimentary geology, edited by: Arthur, M. A., SEPM Short Course, 10, 1–151, 1983.

Bailey, T. R., Rosenthal, Y., Mc Arthur, J. M., Van de Schootbrugge, B., and Thirwall, M. F.: Paleoceanographic changes of the Late Pliensbachian–Early Toarcian interval: a possible link to the genesis of an Oceanic Anoxic Event, Earth Planet. Sci. Lett., 212, 307–320, 2003.

Bassoulet, J. P., Elmi, S., Poisson, A., Ricou, L. E., Cecca, F., Bellion, Y., Guiraud, R., and Baudin, F.: Mid Toarcian (184-182 Ma), in: Atlas Tethys Paleoenvironmental Maps, Explanatory Notes, edited by: Dercourt, J., Ricou, L. E., Vrielynck, B., Gauthier-Villars, Paris, 63–80, 1993.

Bécaud, M., Rulleau, L., and Elmi, S.: Le renouvevellement des faunes d'ammonites à la limite Toarcien moyen-Toarcien supérieur dans les domaines du nord-ouest de l'Europe et de la Téthys occidentale, Bull. Soc. Géol. Fr., 176, 23–35, 2005.

Beerling, D. J., Lomas, M. R., and Gröcke, D. R.: On the nature of methane gas dissociation during the Toarcian and Aptian oceanic anoxic events, Am. J. Sci., 302, 28–49, 2002.

Bonchev, E.: Tectonics of the Fore-Balkan., Bulg. Acad. Sci. Press. Sofia, 1–582, 1971.

Bodin, S., Mattioli, E., Fröhlich, S., Marshall, J. D., Boutib, L., Lahsini, S., and Redfern, J.: Toarcian carbon isotope shifts and nutrient changes from the Northern margin of Gondwana (High Atlas, Morocco, Jurassic): Palaeoenvironmental implications,Palaeogeogr., Palaeoclim., Palaeoecol., 297, 377–390, 2010.

Caruthers, A. H., Gröcke, D. R., and Smith, P. L.: The signi?cance of an Early Jurassic (Toarcian) carbon-isotope excursion in Haida Gwaii (Queen Charlotte Islands), British Columbia, Canada, Earth Planet. Sci. Lett., 307, 19–26, 2011.

Cohen, Å. R.: Geologie des Vorbalkan von Tetewen in Bulgarien nebst die Fauna des Mittleren Lias, Rev. Bulg. Geol. Soc., 3, 15–97, 1931.

Cohen, Å. R.: Die Fauna aus dem oberen Lias, Dogger und Malm des Tetewenbalkan und ihre Bedeutung, Rev. Bulg. Geol. Soc.,4, 3–37, 1932.

Craig, H.: The measurement of oxygen isotope palaeotemperatures, in: Stable isotopes in oceanographic studies and palaeotemperatures, edited by: Tongiorgi, E., Cons. Naz. Rich. Lab. Geol. Nucl., Pisa, Italy, 161–182, 1965.

Dera, G., Pucéat, E., Pellenard, P., Neige, P., Delsate, D., Joachimski, M. M., Reisberg, L., and Martinez, M.: Water mass exchange and variations in seawater temperature in the NW Tethys during the Early Jurassic: Evidence from neodymium and oxygen isotopes of fish teeth and belemnites, Earth Planet. Sci. Lett., 286, 198–207, 2009.

Dera, G., Neige, P., Dommergues J.-L., Fara, E., Laffont, R., and Pellenard, P.: High-resolution dynamics of Early Jurassic marine extinctions: the case of Pliensbachian–Toarcian ammonites (Cephalopoda), J. Geol. Soc. London, 167, 21–33, doi:10.1144/0016-76492009-068, 2010.

Dera, G., Brigaut, B., Monna, F., Laffont, R., Pucéat, E., Deconinck, J.-F., Pellenard, P., Joachimski, M. M., and Durlet, C.: Climatic ups and downs in a disturbed Jurassic world, Geology, 39, 215–218, 2011.

Doyle, P. and Macdonald, D. I. M.: Belemnite battlefields, Lethaia, 26, 65–80, 1993.

Elderfeld, H.: Strontium isotope stratigraphy, Palaeogeogr., Palaeoclim., Palaeoecol., 57, 71–90, 1986.

Elmi, S., Rulleau, L., Gabilly, J., and Mouterde, R.: Toarcien, in: Biostratigraphie du Jurassique ouest-européen et méditerranéen: zonations parallèles et distribution des invertébrés et microfossiles, edited by: Cariou, E. and Hantzpergue, P., Bull. Centre Rech. Explor. Prod. Elf Aquitaine, 17, 25–36, 1997.

Fernández-López, S.: Taphonomic concepts for a theoretical biochronology, Rev. Esp. Paleontol., 6, 37–49, 1991.

Fernández-López, S.: Ammonites, taphonomic cycles and stratigraphic cycles in carbonate epicontinental platforms, Cuad. Geol. Ib., 23, 95–136, 1997.

Fourcade, E., Azéma, J., Bassoulet, J. P., Cecca, F., and Dercourt, J.: Paleogeography and paleoenvironments of the Tethyan Realm during the Jurassic breakup of Pangea, in: The Ocean Basins and Margins, edited by: Nairn, A. E. M., Ricou, L.-E., Vrielynck, B., Dercourt, J., vol. 8: The Tethys Ocean. Plenum Press, New York, 191–214, 1995.

Gómez, J. J. and Goy, A.: Warming-driven mass extinction in the Early Toarcian (Early Jurassic) of northern and central Spain. Correlation with other time-equivalent European sections, Palaeogeogr., Palaeoclim., Palaeoecol., 306, 176–195, 2011.

Gómez, J. J., Goy, A., and Canales, M. L.: Seawater temperature and carbon isotope variations in belemnites linked to mass extinction during the Toarcian (Early Jurassic) in Central and Northern Spain. Comparison with other European sections, Palaeogeogr., Palaeoclim., Palaeoecol., 258, 28–58, 2008.

Gradstein, F. M., Ogg, J. G., and Smith, A. G.: A Geologic Time Scale 2004, Cambridge University Press, Cambridge, 2004.

Gröcke, D. R., Hesselbo, S. P., and Findlay, D. J.: Atypical diagenetic effects on strontium-isotope composition of Early Jurassic belemnites, Queen Charlotte Islands, British Columbia, Canada, Can. J. Earth Sci., 44, 181–197, 2007.

Gröcke, D. R., Hori, R. S., Trabucho-Alexandre, J., Kemp, D. B., and Schwark, L.: An open ocean record of the Toarcian oceanic anoxic event, Solid Earth, 2, 245–257, doi:10.5194/se-2-245-2011, 2011.

Guex, J., Morard, A., Bartolini, A., and Morettini, E.: Découverte d'une importante lacune stratigraphique à la limite Domérien-Toarcien: implications paléoocéanographiques, Bull.Soc. Vaud. Sci. Nat., 345, 277–284, 2001.

Hallam, A. and Bradshaw, M. J.: Bituminous shales and oolithic ironstones as indicators of transgressions and regressions, J. Geol. Soc. London, 136, 157–164, 1979.

Harries, P. J. and Little, C. T. S.: The early Toarcian (Early Jurassic) and the Cenomanian–Turonian (Late Cretaceous) mass extinctions: similarities and contrasts, Palaeogeogr., Palaeoclim., Palaeoecol., 154, 39–66, 1999.

Hesselbo, S. P., Gröcke, D. R., Jenkyns, H. C., Bjerrum, C. J., Farrimond, P., Morgans Bell, H. S., and Green, O. R.: Methane hydrate dissociation during a Jurassic oceanic anoxic event, Nature, 406, 392–395, 2000.

Hesselbo, S. P., Jenkyns, H. C., Duarte, L. V., and Oliveira, L. C. V.: Carbon-isotope record of the Early Jurassic (Toarcian) Oceanic Anoxic Event from fossil wood and marine carbonate (Lusitanian Basin, Portugal), Earth Planet. Sci. Lett., 253, 455–470, 2007.

Izumi, K., Tsuzumi Miyaji, T., and Kazushige Tanabe, K.: Early Toarcian (Early Jurassic) oceanic anoxic event recorded in the shelf deposits in the northwestern Panthalassa: Evidence from the Nishinakayama Formation in the Toyora area, west Japan, Palaeogeogr., Palaeoclim., Palaeoecol., 315/316, 100–108, 2011.

Jenkyns, H. C.: The early Toarcian (Jurassic) anoxic event: stratigraphic, sedimentary and geochemical evidence, Am. J. Sci., 288, 101–151, 1988.

Jenkyns, H. C.: Geochemistry of Oceanic Anoxic Events. Geochem., Geophys., Geosyst., 11, Q03004, doi:10.1029/2009GC002788, 2010.

Jenkyns, H. C. and Clayton, C. J.: Lower Jurassic epicontinental carbonates and mudstones from England and Wales: chemostratigraphic signals and the early Toarcian anoxic event, Sedimentology, 44, 687–706, 1997.

Jenkyns, H. C., Gröcke, D. R., and Hesselbo, S. P.: Nitrogenisotope evidence for watermass denitrification during the early Toarcian (Jurassic) oceanic anoxic event, Paleoceanography, 16, 593–603, 2001.

Jenkyns, H. C., Jones, C. E., Gröcke, D. R., Hesselbo, S. P., and Parkinson, D. N.: Chemostratigraphy of the Jurassic System: applications, limitations and implications for palaeoceanography, J. Geol. Soc. London, 159, 351–378, 2002.

Jones, C. E., and Jenkyns, H. C.: Seawater strontium isotopes, oceanic anoxic events, and seafloor hydrothermal activity in the Jurassic and Cretaceous, Am. J. Sci., 301, 112–149, 2001.

Jones, C. E., Jenkyns, H. C., and Hesselbo, S. P.: Strontium isotopes in Early Jurassic seawater, Geochim. Cosmochim. Acta., 58, 1285–1301, 1994.

Kemp, D. B., Coe, A. L., Cohen, A. S., and Schwark, L.: Astronomical pacing of methane release in the Early Jurassic period, Nature, 437, 396–399, 2005.

McArthur, J. M.: Common on "Carbon-isotope record of the Early Jurassic (Toarcian) Oceanic Anoxic Event from fossil wood and marine carbonate (Lusitanian Basin, Portugal)" by Hesselbo, S., Jenkyns, H. C., Duarte, L. V. and Oliveira, L. C. V., Earth Planet. Sci. Lett., 259, 634–639, 2007.

McArthur, J. M., Donovan, D. T., Thirlwall, M. F., Fouke, B. W., and Mattey, D.: Strontium isotope profile of the early Toarcian (Jurassic) oceanic anoxic event, the duration of ammonite

biozones, and belemnite palaeotemperatures, Earth Planet. Sci. Lett., 179, 269–285, 2000.
Metodiev, L.: The ammonite zones of the Toarcian in Bulgaria – new evidence, subzonation and correlation with the standard zones and subzones in North-western Europe, C. R. Acad. Bulg. Sci., 61, 87–132, 2008.
Metodiev, L. and Koleva-Rekalova, E.: Stable isotope records (δ^{18}O and δ^{13}C) of Lower-Middle Jurassic belemnites from the Western Balkan mountains (Bulgaria): Palaeoenvironmental application, Appl. Geochem., 23, 2845–2856, 2008.
Nachev, I.: Jurassic sedimentary iron ores in the Troyan-Teteven region, Bull. Geol. Inst., 7, 47–103, 1960.
Pálfy, J. and Smith, P. L.: Synchrony between Early Jurassic extinction, oceanic anoxic event, and the Karoo-Ferrar flood basalt volcanism, Geology, 28, 747–750, 2000.
Peterman, Z. L., Hedge, C. E., and Tourtelot, H. A.: Isotopic composition of strontium in sea water throughout Phanerozoic time, Geochim. Cosmochim. Acta, 34, 105–120, 1970.
Rosales, I., Quesada, S., and Robles, S.: Paleotemperature variations of Early Jurassic seawater recorded in geochemical trends of belemnites from the Basque-Cantabrian basin, northern Spain, Palaeogeogr., Palaeoclim., Palaeoecol., 203, 253–275, 2003.
Rosales, I., Robles, S., and Quesada, S.: Elemental and oxygen isotope composition of Early Jurassic belemnites: Salinity vs. temperature signals, J. Sed. Res., 74, 342–354, 2004.
Ruget, C. and Nicollin, J.-P.: Foraminifères, in: Biostratigraphie du Jurassique ouest-européen et méditerranéen: zonations parallèles et distribution des invertébrés et microfossiles, edited by: Cariou, E. and Hantzpergue, P., Bull. Centre Rech. Explor. Prod. Elf Aquitaine, 17, 281–291, 1997.
Sapunov, I.: Stratigraphy of the Jurassic in the Etropole and Teteven areas (Central Balkan Range), Trav. géol. Bulg., sér. stratigr. et tect., 3, 93–137, 1961.
Sapunov, I.: The ammonite zones of the Toarcian in Bulgaria, Bull. Geol. Inst., 17, 133–165, 1968.
Sapunov, I.: On certain recent stratigraphic problems of the Jurassic System in Bulgaria, Bull. Geol. Inst., 18, 5–20, 1969.
Sapunov, I. and Tchoumatchenco, P.: Some new concepts on the lithostratigraphy of the Middle Jurassic marine sediments in West and Central Bulgaria, Rev. Bulg. Geol. Soc., 50, 15–25, 1989.
Sapunov, I., Tchoumatchenco, P., and Shopov, V.: Concerning certain features of the palaeogeography of the Teteven Area in the Early Jurassic. Bull. Geol. Inst., 20, 33–62 1971.

SED
4, 315–361, 2012

Toarcian belemnite isotope study from Bulgaria

L. S. Metodiev et al.

Sælen, G., Doyle, P., and Talbot, M.: Stable-isotope analyses of belemnite rostra from the Whitby Mudstone Fm., England: Surface water conditions during deposition of a marine black shale, Palaios, 11, 97–117, 1996.
Shopov, V.: Bivalvian zones in the lower Jurassic in Bulgaria, Bull. Geol. Inst., 19, 15–39, 1970.
Shackleton, N. J. and Kennett, J. P.: Paleotemperature history of the Cenozoic and the initiation of Antarctic glaciation: oxygen and carbon isotope analyses in DSDP Sites 277, 279, and 281, in: Initial Reports, edited by: Kennett, J. P., Houtz, R. E, et al., DSDP, 29, 743–755 US Government Printing Office, Washington, 1975.
Schouten, S., van Kaam Peters, H., Rijpstra, W. I. C., Schoell, M., and Sinninghe Damste, J: Effectsof an oceanic anoxic event on the stablecarbon isotopic composition of Early Toarciancarbon, Am. J. Sci., 300, 1–22, 2000.
Suan, G., Mattioli, E., Pittet, B., Lécuyer, C., Suchéras-Marx, B., Duarte, L. V., Philippe, M., Reggiani, L., and Martineau, F.: Secular environmental precursors of Early Toarcian (Jurassic) extreme climate changes, Earth Planet. Sci. Lett., 290, 448–458, 2010.
Suan, G., Nikitenko, B. L., Rogov, M. A., Baudin, F., Spangenberg, J. E., Knyazev, V. G., Glinskikh, L. A., Goryacheva, A. A., Adatte, T., Riding, J. B., Föllmi, K., Pittet, B., Mattioli, E., and Lécuyer, C.: Polar record of Early Jurassic massive carbon injection, Earth Planet. Sci. Lett., 312, 102–113, 2011.
Svensen, H., Planke, S., Chevallier, L., Malthe-Sorenssen, A., Corfu, F., and Jamtveit, B.: 30 Hydrothermal venting of greenhouse gases triggering Early Jurassic global warming, Earth Planet. Sci. Lett., 256, 554–566, 2007.
Toula, F.: Grundlinien der Geologie des westlichen Balkan, Denkschr. k. Akad. Wissensch., mathem.-naturwiss.,44, 1–56, 1881.
Toula, F.: Geologische Untersuchungen im centralen Balkan, Denkschr. k. Akad. Wissensch., mathem.-naturwiss.,55, 1–108, 1889.
Tremolada, F., van de Schootbrugge, B., and Erba, E.: Early Jurassic schizosphaerellid crisis in Catabria, Spain: implications for calcification rates and phytoplankton evolution across the Toarcian oceanic anoxic event, Paleoceanography, 20, PA2011, doi:10.1029/2004PA001120, 2005.
van Buchem, F. S. P., Knox, R. W. O'B.: Lower and Middle Liassic depositional sequences of Yorkshire (U.K.), In Mesozoic and Cenozoic Sequence Stratigraphy of the European Basins, edited by: de Graciansky, P. C., Hardenbol, J., Jacquin, T., and Vail, P. R., SEPM Special Publications, 60, 545–559, 1998.

van de Schootbrugge, B., McArthur, J. M., Bailey, T. R., Rosenthal, Y., Wright, J. D., and Miller, K. G.: Toarcian oceanic anoxic event: An assessment of global causes using belemniteisotope records, Paleoceanography, 20, PA3008, doi:10.1029/2004PA001102, 2005.
van Houten, F. B. and Purucker, M. E.: Glauconitic peloids and chamositic ooids – favorable factors, constrains and problems, Earth Sci. Rev., 20, 211–243, 1984.
Veizer, J., Buhl, D., Deine, A., Ebneth, S., Podlaha, O. G., Bruckschen, P., Jasper, T., Korte, C., Schaaf, M., Ala, D., and Azmy, K.: Strontium isotope stratigraphy: potential resolution and event correlation, Palaeogeogr. Palaeoclim. Palaeoecol., 132, 65–77, 1997.
Waltham, D. A. and Gröcke, D. R.: Non-uniqueness and interpretation of the seawater $^{87}Sr/^{86}Sr$ curve, Geochim. Cosmochim. Acta, 70, 384–394, 2006.
Wignall, P. B., Newton, R. J., and Little, C. T. S.: The timing of paleoenvironmental change and cause-and-effect relationships during the early Jurassic mass extinction in Europe, Am. J. Sci., 305, 1014–1032, 2005.
Wignall, P. B., McArthur, J. M., Little, C. T. S., and Hallam, A.: Palaeoceanography: Methane release in the Early Jurassic period, Nature, 441, E5, doi:10.1038/nature04905, 2006.
Young, T. P.: Phanerozoic ironstones: an introduction and review. in: Phanerozoic ironstones, edited by: Young, T. P. and Taylor, W. E., Geol. Soc. Special Pub., 46, ix-xxv, 1989.
Zagorchev, I., Dabovski, H., and Nikolov, T.: Geology of Bulgaria. Vol. II. Mesozoic geology. Prof. M. Drinov Acad. Press. Sofia. 766 pp., 2009.
Zlatarski, G.: Le système jurassique en Bulgarie, Ann. Univ. Sofia. 3, 148–224, 1908.

Table 1. Isotope data for belemnites collected from the Toarcian of Varbanchovets section (Central Fore-Balkan), Bulgaria.

No.	Sample ID	Bed No.	Ammonite zone (*subzone*)	Numerical age	$^{87}Sr/^{86}Sr$	Std error (Abs)	$\delta^{13}C$ (VPDB)	$\delta^{18}O$ (VPDB)	PalaeoT(°C) calculated
1.	V-26	5	Fallaciosum	180.94	0.707270	7.1×10^{-6}	1.43	−2.53	22.6°
2.	V-25	4	Thouarsense	181.04	0.707295	6.9×10^{-6}	1.91	−2.35	21.8°
3.	V-24	4	Thouarsense	181.20	0.707312	6.5×10^{-6}	1.21	−2.21	21.2°
4.	V-23	4	Variabilis	181.23	0.707236	5.8×10^{-6}	1.24	−1.46	17.9°
5.	V-22	4	Variabilis	181.33	0.707245	2.5×10^{-6}	0.84	−1.79	19.4°
6.	V-21	4	Variabilis	181.43	0.707238	$4.7\times1\ 0^{-6}$	1.61	−1.58	18.4°
7.	V-20	3c	Bifrons (*Semipolitum*)	181.44	0.707233	3.4×10^{-6}	1.34	−2.56	22.8°
8.	V-19	3c	Bifrons (*Semipolitum*)	181.48	0.707343	4.8×10^{-6}	1.72	−2.99	24.8°
9.	V-18	3c	Bifrons (*Bifrons*)	181.52	0.707224	3.2×10^{-6}	1.87	−2.03	20.4°
10.	V-17	3c	Bifrons (*Bifrons*)	181.56	0.707234	4.4×10^{-6}	1.35	−2.16	21.0°
11.	V-16	3c	Bifrons (*Bifrons*)	181.61	0.707229	1.3×10^{-6}	2.48	−2.26	21.4°
12.	V-15	3c	Bifrons (*Lusitanicum*)	181.66	0.707217	5.4×10^{-6}	1.60	−2.07	20.6°
13.	V-14	3b	Bifrons (*Lusitanicum*)	181.71	0.707244	3.5×10^{-6}	1.11	−2.62	23.1°
14.	V-13	3b	Bifrons (*Lusitanicum*)	181.81	0.707232	2.7×10^{-6}	1.62	−2.97	24.7°
15.	V-12	3a	Bifrons (*Lusitanicum*)	181.81	0.707388*	4.4×10^{-6}	1.23	−3.75	28.4°
16.	V-11	2	Falciferum	182.32	0.707153	4.6×10^{-6}	2.51	−1.93	20.0°
17.	V-10	2	Falciferum	182.70	0.707132	4.9×10^{-6}	1.10	−1.61	18.6°
18.	V-9	2	Falciferum	183.07	0.707101	$4.8\times1\ 0^{-6}$	3.21	−1.59	18.5°
19.	V-8	1d	Tenuicostatum (*Semicelatum*)	183.30	0.707164	3.9×10^{-6}	2.60	−2.62	23.1°
20.	V-7	1d	Tenuicostatum (*Semicelatum*)	183.30	0.707134	4.8×10^{-6}	2.90	−1.62	18.6°
21.	V-6	1d	Tenuicostatum (*Semicelatum*)	183.31	0.707111	5.6×10^{-6}	2.31	−1.11	16.5°
22.	V-5	1c	Tenuicostatum (*Semicelatum*)	183.31	0.707108	5.1×10^{-6}	3.25	−1.38	17.6°
23.	V-4	1b	Tenuicostatum (*Semicelatum*)	183.33	0.707371*	5.0×10^{-6}	2.21	−2.61	23.0°
24.	V-3	1b	Tenuicostatum (*Semicelatum*)	183.34	0.707088	4.6×10^{-6}	1.35	−0.81	15.2°
25.	V-2	1a	Tenuicostatum (*Semicelatum*)	183.35	0.707154	7.0×10^{-6}	2.20	−0.73	14.9°
26.	V-1	1a	Tenuicostatum (*Semicelatum*)	183.36	0.707177	4.06×10^{-6}	0.95	−1.73	19.1°

*For clarity the $^{87}Sr/^{86}Sr$ ratios of samples V-4 and V-12 are not shown on the curve on Fig. 3, because of their very radiogenic values that plot outside the general trend. However, these values appear to coincide with prominent palaeotemperature rises, calculated in the middle of the Semicelatum Subzone and at the base of the Bifrons Zone.

SED
4, 315–361, 2012

Table 2. Isotope data for belemnites collected from the Pliensbachian and the Toarcian of Babintsi section (Central Fore-Balkan), Bulgaria.

No.	Sample ID	Pack No.	Ammonite zone (*subzone*)	Numerical age	$^{87}Sr/^{86}Sr$	Std error (Abs)	$\delta^{13}C$ (VPDB)	$\delta^{18}O$ (VPDB)	PalaeoT (°C) calculated
1.	Ba-22	3b	Fallaciosum	180.92	0.707323	3.9×10^{-6}	0.90	−3.13	25.4°
2.	Ba-21	3a	Thouarsense	181.06	0.707291	4.5×10^{-6}	−0.66	−1.73	19.1°
3.	Ba-20	3a	Thouarsense	181.15	0.707349	4.7×10^{-6}	−0.40	−2.53	22.6°
4.	Ba-19	3a	Thouarsense	181.22	0.707310	4.9×10^{-6}	0.05	−1.85	19.6°
5.	Ba-18	3a	Variabilis	181.24	0.707220	4.2×10^{-6}	2.38	−2.36	21.9°
6.	Ba-17	3a	Variabilis	181.27	0.707248	7.2×10^{-6}	1.70	−2.49	22.2°
7.	Ba-16	3a	Variabilis	181.30	0.707311	4.4×10^{-6}	1.10	−3.36	26.5°
8.	Ba-15	3a	Variabilis	181.33	0.707260	4.0×10^{-6}	2.34	−1.77	19.3°
9.	Ba-14	3a	Variabilis	181.36	0.707269	4.2×10^{-6}	1.03	−1.84	19.6°
10.	Ba-13	3a	Variabilis	181.39	0.707219	7.0×10^{-6}	2.11	−1.69	18.9°
11.	Ba-12	3a	Variabilis	181.42	0.707236	4.0×10^{-6}	1.25	−2.08	20.6°
12.	Ba-11	2c	Bifrons (*Semipolitum*)	181.45	0.707227	6.4×10^{-6}	2.03	−2.04	20.5°
13.	Ba-10	2c	Bifrons (*Bifrons*)	181.52	0.707214	4.0×10^{-6}	0.43	−1.96	20.1°
14.	Ba-9	2c	Bifrons (*Bifrons*)	181.54	0.707216	5.1×10^{-6}	0.88	−1.88	19.7°
15.	Ba-8	2c	Bifrons (*Bifrons*)	181.59	0.707256	7.8×10^{-6}			
16.	Ba-7	2b	Bifrons (*Lusitanicum*)	181.64	0.707251	5.1×10^{-6}	1.12	−2.07	20.6°
17.	Ba-6	2b	Bifrons (*Lusitanicum*)	181.67	0.707243	5.9×10^{-6}	1.68	−2.18	21.0°
18.	Ba-5	2a	Bifrons (*Lusitanicum*)	181.80	0.707230	3.9×10^{-6}	2.69	−2.19	21.1°
19.	Ba-4	2a	Upper Pliensbachian	184.27	0.707087	4.6×10^{-6}	0.59	−2.68	23.3°
20.	Ba-3	2a	Upper Pliensbachian	184.37	0.707115	9.9×10^{-6}	2.03	−0.30	13.2°
21.	Ba-2	2a	Upper Pliensbachian	184.47	0.707134	4.7×10^{-6}	0.20	−2.42	22.1°
22.	Ba-1	2a	Upper Pliensbachian	184.66	0.707130	6.4×10^{-6}	1.63	0.43	9.8°

SED
4, 315–361, 2012

Toarcian belemnite isotope study from Bulgaria

L. S. Metodiev et al.

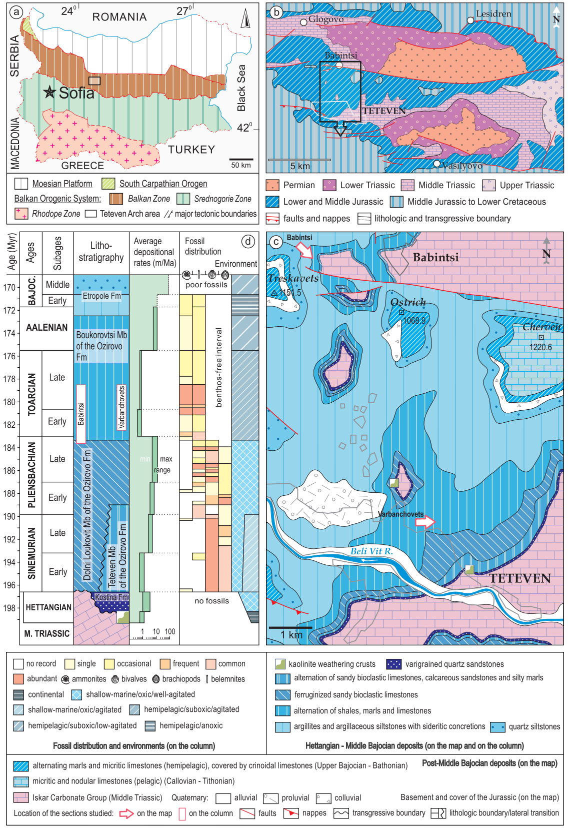

Fig. 1. Location of the sections used for this study. **(a)** Simplified tectonic sketch showing position of the Teteven Arch within the framework of the Balkan Orogenic System and its foreland in Bulgaria; **(b)** Geological sketch map of the Teteven Arch (Central Fore-Balkan, Bulgaria) with the area containing sections Varbanchovets and Babintsi; **(c)** Geological map of the area around the town of Teteven; **(d)** Generalized lithostratigraphic scheme of the Lower and the Middle Jurassic deposits on the geological map with positions of sections sampled, and the average depositional rates of Early-Middle Jurassic ages calculated on the time-scale of Gradstein et al. (2004), relative distribution of major fossil groups (modified after Sapunov et al., 1971), and related depositional environments.

SED

4, 315–361, 2012

Toarcian belemnite isotope study from Bulgaria

L. S. Metodiev et al.

Title Page

Abstract | Introduction

Conclusions | References

Tables | Figures

◀| |▶

◀ ▶

Back | Close

Full Screen / Esc

Printer-friendly Version

Interactive Discussion

Substage	Bulgaria (after Metodiev, 2008)		North-West Europe (after Elmi et al., 1997)		Substage
	Zone	Subzone	Subzone	Zone	
Upper Toarcian (Yeovilian)	Aalensis	Aalensis	Lugdunensis	Aalensis	Upper Toarcian
		Mactra	Mactra		
	Pseudoradiosa	Pseudoradiosa	Pseudoradiosa	Pseudoradiosa	
		Levesquei	Levesquei		
	Dispansum		Gruneri	Dispansum	
			Insigne		
	Fallaciosum		Fallaciosum	Thouarsense	
	Thouarsense	Fascigerum	Fascigerum		
		Thouarsense	Thouarsense		
		Bingmanni	Bingmanni		
	Variabilis	Denckmannia	Vitiosa	Variabilis	Middle Toarcian
			Illustris		
		Collina	Variabilis		
Lower Toarcian (Whitbian)	Bifrons	Semipolitum	Bifrons	Bifrons	
		Bifrons			
		Lusitanicum	Sublevisoni		
	Falciferum	Falciferum	Falciferum	Serpentinum	Lower Toarcian
		Serpentinum	Elegantulum		
	Tenuicostatum	Semicelatum	Semicelatum	Tenuicostatum	
		Crosbeyi	Paltum		

Fig. 2. Approximate correlation between the ammonite biostratigraphy for the Toarcian in Bulgaria and that of north-western Europe. The grey area on the table indicates the zones and subzones determined by the ammonite occurrence of the studied sections.

SED
4, 315–361, 2012

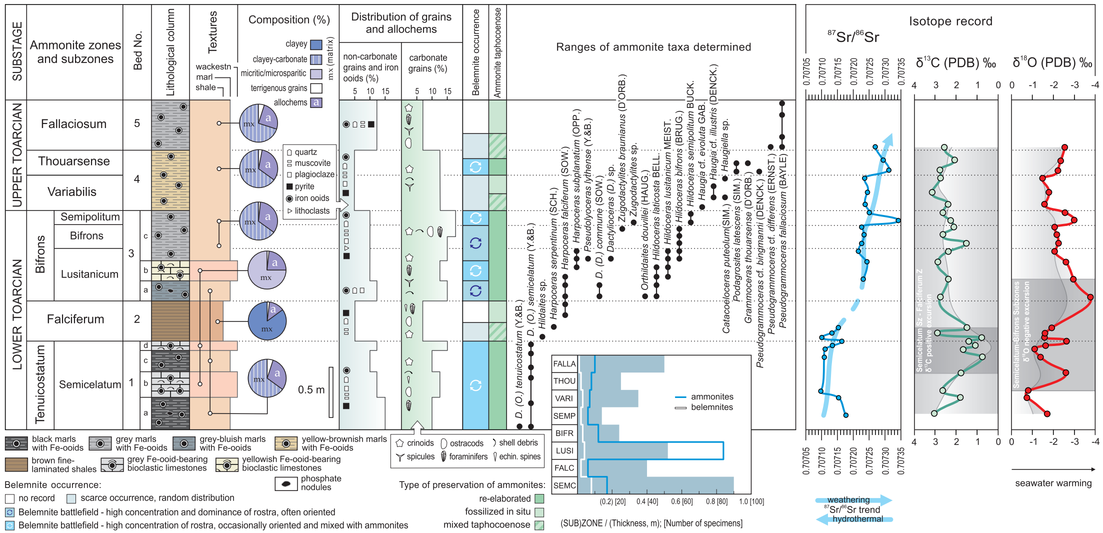

Fig. 3. Stratigraphic log of the Toarcian sediments of section Varbanchovets. The ammonite biostratigraphic subdivision is represented against the fossil-bearing lithological succession, given as column, composition, and distribution of grains and allochems of the rocks. The pattern of distribution of belemnite rostra through the section and types of preservation of ammonite associations are shown, linked with a chart of ranges of the ammonite taxa determined, as well as the $^{87}Sr/^{86}Sr$, the $\delta^{13}C$, and the $\delta^{18}O$ curves obtained after the measurements on belemnites. The small diagram below the fossil range-chart represents the fossil-empirical basement of the study of this section: thickness of the zones/subzones, number of ammonites collected and belemnites analyzed from each unit. Zones/subzones abbreviations: SEMC–Semicelatum, FALC–Falciferum, LUSI–Lusitanicum, BIFR–Bifrons, SEMP–Semipolitum, VARI–Variabilis, THOU–Thouarsense, FALLA–Fallaciosum.

SED
4, 315–361, 2012

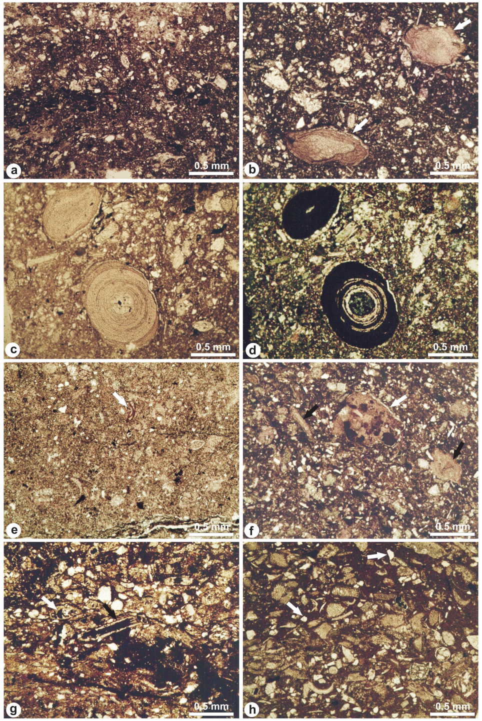

Fig. 4. Microphotographs of the rocks from section Varbanchovets. **(a)** Marl with carbonate-clayey matrix containing poorly sorted and randomly dispersed broken skeletal grains, rare clastic grains (quartz, feldspars) and pyrite; Bed No. 5, PPL. **(b)** Marls composed of bioclasts, clastic non-carbonate grains and deformed phosphatized ferruginous ooids (white arrows) dispersed within carbonate-clayey matrix; Bed No. 4, PPL. **(c),** and **(d)** Plane- and cross-polarized light microphotographs of phosphatized and partly carbonatized ferruginous ooids; Bed No. 3c. **(e)** Bioclastic wackestone containing recrystallized biodetritus and sporadic foraminifers (white arrow); Bed No. 3b, PPL. **(f)** Marl with phosphate nodule (white arrow) and deformed phosphatized ooids (black arrows); Bed No. 3a, PPL. **(g)** Ferruginous shale composed of ferruginous clayey matrix and bioclasts – echinoid spines (black arrow), foraminifers (white arrow), ostracods, and crinoids. Clastic non-carbonate grains also occur; Bed No. 2, PPL;**(h)** Marl containing poorly sorted biodetritus (crinoids, brachiopods, echinoids, thin-shelled ostracods and foraminifers) and clastic quartz and feldspar grains (white arrows) presented within calcareous-clayey matrix; Bed No. 1c, PPL.

SED
4, 315–361, 2012

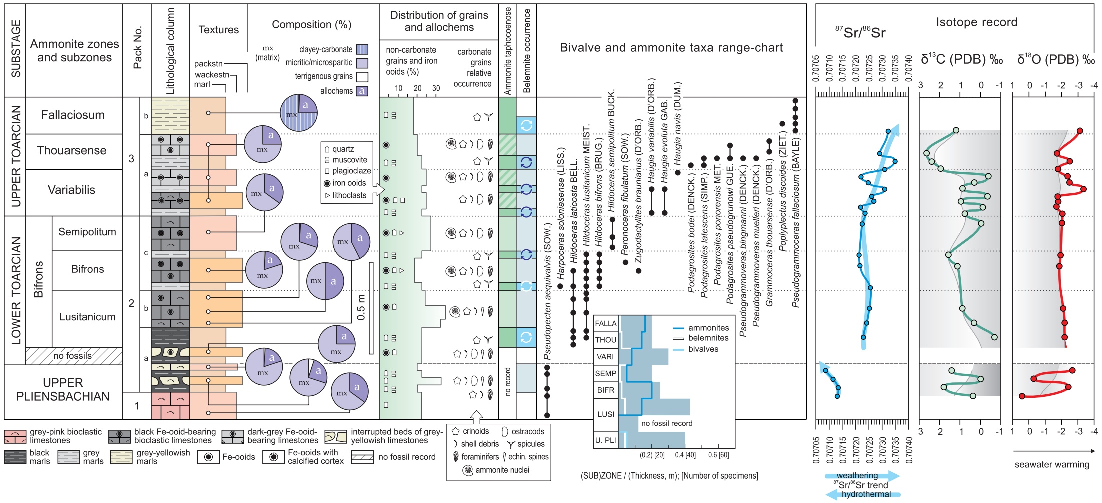

Fig. 5. Stratigraphic log of the Uppermost Pliensbachian and the Toarcian sediments of section Babintsi. The ammonite biostratigraphic subdivision is represented against the fossil-bearing lithological succession, given as column, composition, and distribution of grains and allochems of the rocks. Belemnite occurrence through the section, the types of preservation of ammonite associations, range-chart of the bivalve and ammonite taxa determined, and the $^{87}Sr/^{86}Sr$, the $\delta^{13}C$, and the $\delta^{18}O$ curves obtained after the measurements on belemnites collected are given as well. The aim of the diagram below the fossil range-chart and abbreviations used, as well as symbols for belemnite distribution and ammonite taphocoenoses, are the same as in Fig. 3.

SED
4, 315–361, 2012

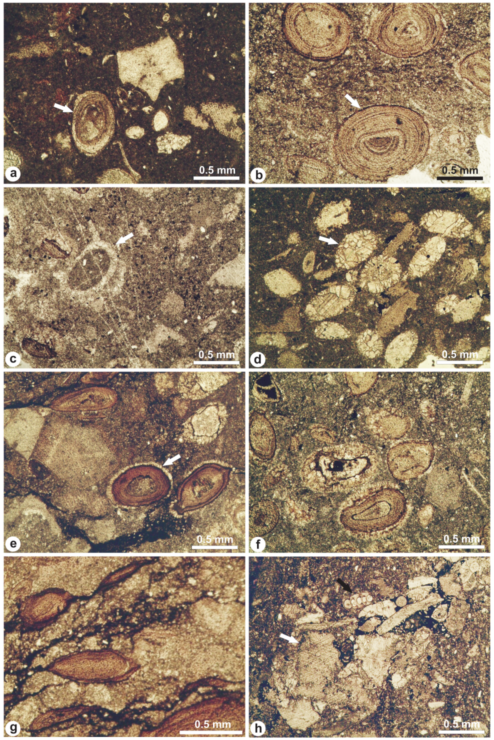

Fig. 6. Microphotographs of the rocks from section Babintsi. **(a)** Bioclastic wackestone composed of poorly sorted and randomly dispersed skeletal grains (mostly crinoids and rare shell debris), partly carbonatized ferruginous ooids (white arrow), and clay-rich micritic matrix. Pack No. 3a, PPL. **(b)** Ferruginous ooids with normal cortices and well-preserved concentric layering. Some ooid nuclei are presented by other broken ooid individuals (white arrow). Pack No. 3a, PPL. **(c)** Bioclastic wackestone containing crinoid fragments, gastropod shells (white arrow) and ferruginous ooids. Pack No. 2c, PPL. **(d)** Completely carbonatized ferruginous ooids (white arrow) associating with bioclasts. Pack No. 2c, PPL. **(e)** Bioclastic wackestone with ferruginous ooids. External parts of some ooid cortices are built up of carbonate layers with radial microfabric (white arrow). Pack No. 2b, PPL. **(f)** Carbonatized in various degree ferruginous ooids. Pack No. 2b, PPL. **(g)** Distorted ooid individuals. Pack No. 2b, PPL. **(h)** Bioclastic wackestone/packstone containing poorly sorted bioclasts of crinoids (white arrow), shell debris and foraminifers (black arrow). Pack No. 2a, PPL.

SED
4, 315–361, 2012

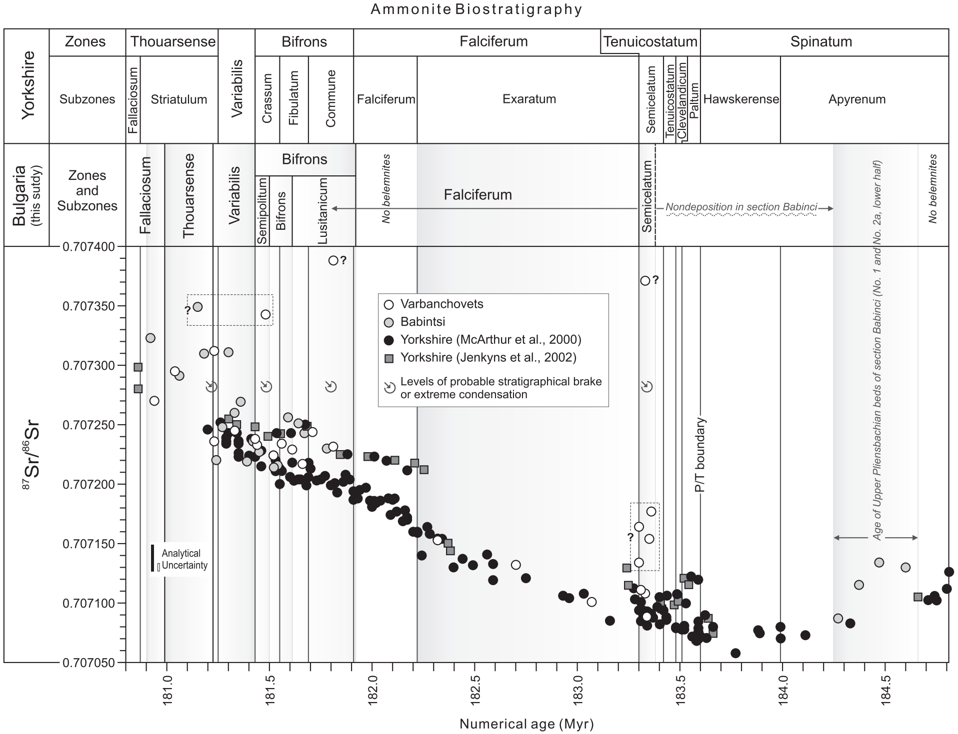

Fig. 7. Belemnite $^{87}Sr/^{86}Sr$ isotope ratios versus calculated numerical age in millions of years (Myr) for the Bulgarian sections (Varbanchovets and Babintsi, this study), and the Jurassic sections of the Yorkshire coast, UK (values from McArthur et al., 2000 and Jenkyns et al., 2002). To make comparisons easier, all of the reported Sr isotope ratios in the Bulgarian and in the UK Jurassic sections have been normalized to the same NIST 987 $^{87}Sr/^{86}Sr$ values of 0.710248. The duration of the various ammonite biozones (shown on top) have been calculated following the methods outlined in detail in McArthur et al. (2000). Overall it appears that the duration of the ammonite biozones in Bulgaria confirms the results from the UK sections. Exceptions are the Fallaciosum and the Semicelatum subzones, which in the Bulgarian sections appear to be longer and shorter, respectively. Although the analytical uncertainty of the Bulgarian section is better (note that the filled vertical bar is for the UK data and the white vertical bar is for the Bulgarian section), please note that the belemnite sampling/density in the Bulgarian sections is much lower and that there are a few samples containing elevated $^{87}Sr/^{86}Sr$ ratios, although those were not included in the calculation of the numerical ages.

SED
4, 315–361, 2012

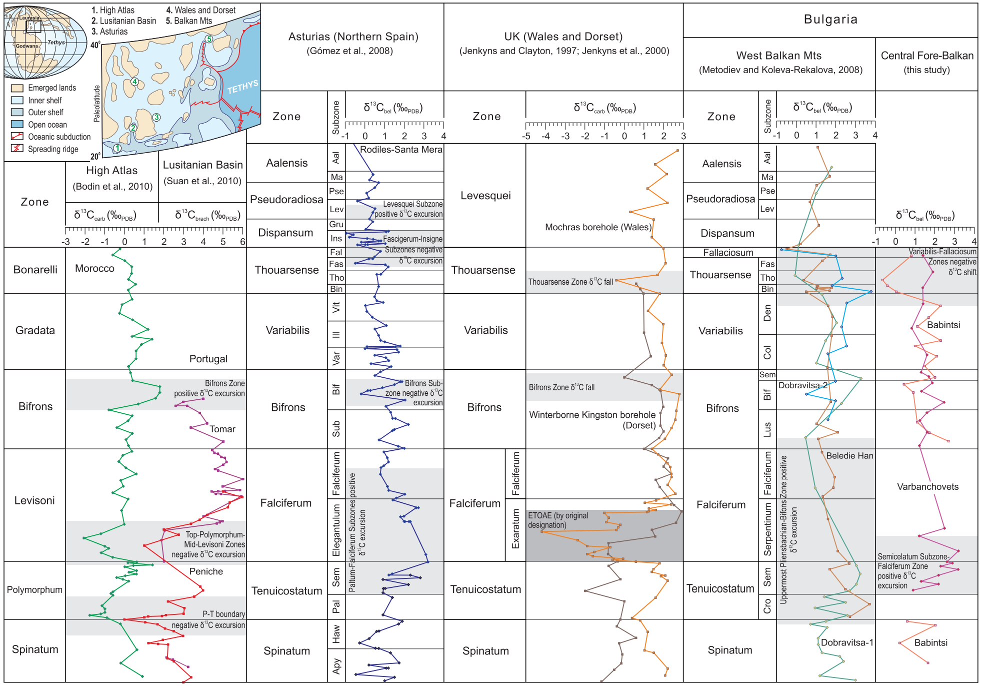

Fig. 8. Correlation of the carbon isotope record from the sections of the Central Fore-Balkan, Bulgaria (this study), the sections from the West Balkan Mountains (Bulgaria; Metodiev and Koleva-Rekalova, 2008), the Ammelago section (High Atlas, Morocco; Bodin et al., 2010), sections Tomar and Peniche (Lusitanian Basin, Portugal; Suan et al., 2010), Asturias (Northern Spain; Gómez et al., 2008), and Mochras and Winterborne Kingston boreholes (Wales and Dorset, UK; Jenkyns and Clayton, 1997, Jenkyns et al., 2001). The grey bands on each section indicate intervals of prominent δ^{13}C excursions. The upper left corner represents palaeogeographical sketch of the Western part of the Tethyan Realm during the Toarcian (simplified and modified after Metodiev and Koleva-Rekalova (2008), based upon the references cited therein) with the approximate locations of the sections compared.

SED
4, 315–361, 2012

Toarcian belemnite isotope study from Bulgaria

L. S. Metodiev et al.

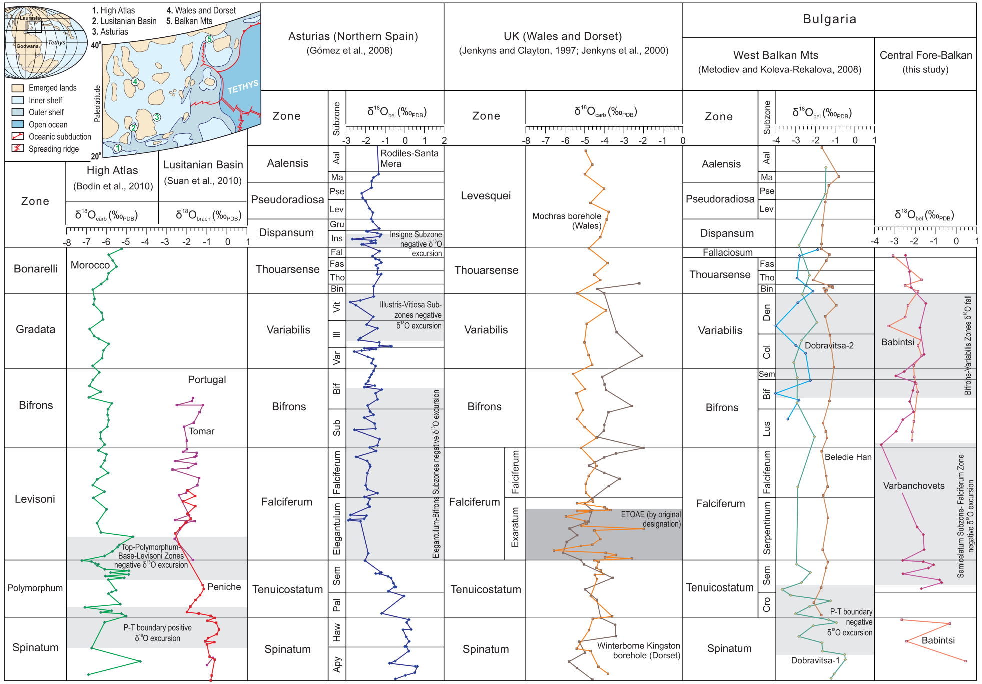

Fig. 9. Correlation of the oxygen isotope record from the sections of the Central Fore-Balkan, Bulgaria (this study), the sections from the West Balkan Mountains (Bulgaria; Metodiev and Koleva-Rekalova, 2008), the Ammelago section (High Atlas, Morocco; Bodin et al., 2010), sections Tomar and Peniche (Lusitanian Basin, Portugal; Suan et al., 2010), Asturias (Northern Spain; Gómez et al., 2008), and Mochras and Winterborne Kingston boreholes (Wales and Dorset, UK; Jenkyns and Clayton, 1997, Jenkyns et al., 2001). The grey bands of each section indicate intervals of prominent $\delta^{18}O$ excursions. The upper left corner represents palaeogeographical sketch of the Western part of the Tethyan Realm during the Toarcian (simplified and modified after Metodiev and Koleva-Rekalova (2008), based upon the references cited therein) with the approximate locations of the sections compared.

SED
4, 315–361, 2012

Toarcian belemnite isotope study from Bulgaria

L. S. Metodiev et al.

Title Page
Abstract | Introduction
Conclusions | References
Tables | Figures
◀| |▶
◀ ▶
Back | Close
Full Screen / Esc
Printer-friendly Version
Interactive Discussion